Cancer Management and Research

Elevate Series

Open Access Full Text Article

REVIEW

The Role of Artificial Intelligence and Radiomics in the Management of Lymphomas by PET/CT: The Clairvoyance in Clinic

Chong ling Duan[1,*], Lin An[1,*], Yong feng Yang[1], Lili Yuan[1], Yandong Zhu[1], Qian Han[1], Hongbing Ma[1], Fei Zhao[1], Qing-qing Yu[2]

[1]Jining No.1 People's Hospital, Shandong First Medical University, Jining, People's Republic of China; [2]Clinical Research Center, Jining No. 1 People's Hospital, Shandong First Medical University, Jining, People's Republic of China

*These authors contributed equally to this work

Correspondence: Qing-qing Yu, Clinical Research Center, Jining No.1 People's Hospital, Shandong First Medical University, Jining, People's Republic of China, Email yuqingqing_lucky@163.com

Abstract: Lymphomas are a hematopoietic malignancies that encompass over 90 subtypes. Traditionally, they have been categorized into two main groups, non-Hodgkin lymphoma (NHL) and Hodgkin lymphoma (HL). Based on morphology and immunohistochemistry, HL can be classified into nodular lymphocyte-predominant Hodgkin lymphoma (NLPHL) and classical HL (cHL). NHL represents the most common form of lymphoma, including more than 50 subtypes, such as mantle cell lymphoma (MCL), follicular lymphoma (FL), marginal zone lymphoma (MZL), and the most common, diffuse large B-cell lymphoma (DLBCL). Medical imaging plays a pivotal role in lymphoma management, with positron emission tomography/computed tomography (PET/CT) serving as an indispensable tool. 2-Deoxy-2-[fluorine-18]fluoro-D-glucose (18F-FDG) PET/CT is extensively utilized in lymphoma management, having demonstrated its value in providing crucial data for precise disease burden quantification, treatment response evaluation, and prognostic assessment. Radiomics is an innovative approach that entails the computer-aided extraction of quantitative, searchable data from medical images and its association with biological and clinical outcomes. The rapid advancement of radiomics research has opened new avenues for cancer diagnosis and therapy. Our findings indicate that artificial intelligence based PET/CT radiomics has demonstrated significant potential in lymphoma diagnosis, subtyping, staging, treatment selection, and survival prognosis assessment, offering clinicians powerful decision-support tools. However, challenges remain, such as the lack of standardized image quality in machine learning applications.

Keywords: lymphomas, PET/CT, radiomics, imaging, artificial intelligence

Introduction

Lymphoma is a malignancy of the hematopoietic system. Over the past two decades, there has been a significant global increase in lymphoma incidence. According to the Global Cancer Statistics approximately 20.0 million new cancer cases were diagnosed worldwide in 2022, including 0.08 million cases of HL and 0.5 million cases of NHL. Among the 9.73 million cancer-related deaths, lymphoma accounted for 0.27 million (2.8%), establishing it as a principal cause of cancer mortality.[1] Lymphoma biology and clinical manifestations are heterogeneous.[2] Lymphoma usually presents as painless lymph node enlargement, but it can also occur without obvious symptoms, leading to misdiagnosis. Although survival rates for lymphoma patients have improved in recent decades, there are still wide variations in five-year survival rates. The high heterogeneity and misdiagnosis rates of lymphoma highlight the urgency of developing non-invasive, effective diagnostic tools. Medical imaging research is essential for optimizing lymphoma diagnosis and treatment.

Lymphoma is a highly heterogeneous tumor.[3–5] Tumor heterogeneity reflects the characteristics of tumor growth and biology.[6,7] It serves as a crucial prognostic marker for assessing cancer progression, relapse potential, and treatment resistance.[8–10] Lymphoma is not limited to the lymphatic system, but extends widely to various parts of the body, including solid organs (e.g., liver and lungs), soft tissues, and bone marrow.[11,12] In clinical practice, biopsy or lesion resection is usually performed on a single lesion site, meaning that insufficient heterogeneity reflects the whole tumor and information can only be

Received: 27 March 2025
Accepted: 9 July 2025
Published: 19 July 2025

acquired from a scant few sites, perhaps even just one.[13] Additionally, this approach is highly invasive, non-repeatable,[14–16] and may cause complications. Recently, several studies have clearly shown that radiomics shows substantial potential for non-invasive assessment of tumor heterogeneity.[17–20] This methodology employs sophisticated high-dimensional analysis of imaging data to effectively characterize tumor heterogeneity,[17,18] thereby offering robust reinforcement for the prognosis of clinical outcomes.[21] Its advantage is that it can realize non-invasive, real-time, dynamic, and reproducible monitoring of tumor, which opens up a new way for tumor diagnosis and treatment.[22] Artificial intelligence (AI) is developing rapidly. Studies increasingly prove that integrating AI with MRI,[23] pathology,[24] and genetic data[25] is important for lymphoma diagnosis and treatment. Particularly, PET/CT imaging—a crucial molecular imaging technology—offers important advantages when combined with AI. Based on existing lesion morphological features, PET/CT radiomics incorporates first-order, second-order, and higher-order features, alongside the characteristic metabolic features of PET, in order to more accurately depict tumor heterogeneity.[26–28] This paper aims to investigate the role of AI-assisted PET/CT radiomics in lymphoma management, including diagnosis, subtyping, staging, risk stratification, treatment selection, and prognosis prediction. Additionally, we discuss key methodological aspects such as radiomic feature extraction, model comparative analysis, and advanced deep learning techniques.

Radiomics and Artificial Intelligence

PET/CT radiomics can extract detailed tissue and lesion features from medical images.[29–31] These features can be used either independently or in conjunction with demographic, histological, genomics, or proteomic data to predict the underlying biological properties and tumors' biological behavior, thereby elucidating the correlation between patients' clinical characteristics and prognosis.[32–34] The basic workflow of PET/CT imaging radiomics comprises: acquiring and standardizing images, region labeling, segmenting the images, calculating and selecting features, reducing dimensionality, constructing the model, and finally, evaluating the model (Figure 1).

Radiomics features (RF) are generally classified into statistical features, encompassing histogram-based feature and texture-based features; model-based feature; transform-based feature; and shape-based feature.[35] Histogram features (also called first-order features) represent the most basic statistical descriptors. Derived from individual pixel or voxel analysis without incorporating spatial information, these features mainly include mean, maximum, minimum, variance, and percentiles of the gray levels.[36] In PET imaging, the routinely used SUV measurements—SUV max, SUV mean, and SUV peak—all represent first-order

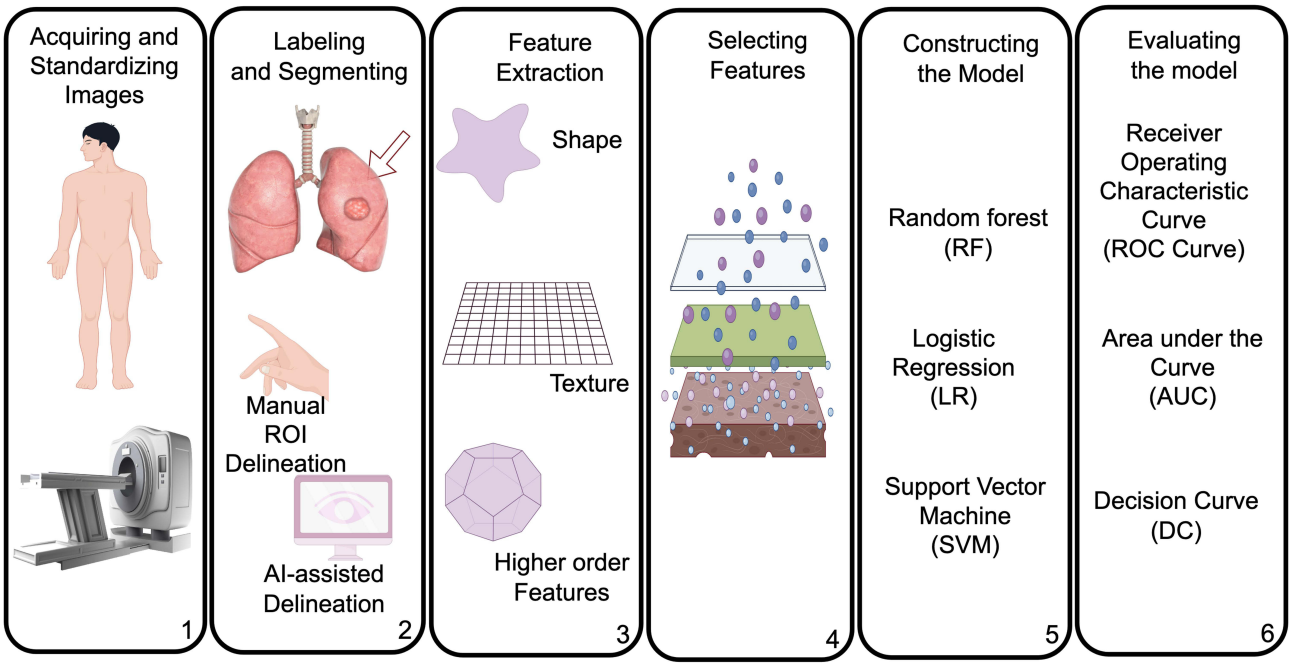

Figure 1 The picture depicts the workflow of radiomics. (1) Image acquisition and standardization, (2) Labeling and segmentation, (3) Feature extraction, (4) Feature selection, (5) Model construction, (6) Model evaluation.

features. Texture features, also known as second-order features, characterize the spatial organization and intensity hierarchy of voxels, serving as one of the conventional methods for quantifying tumor heterogeneity.[37] The most commonly utilized second-order features include GLCM, GLRLM, GLSZM, GLDZM, NGTDM, and the NGLDM.[38] Model-based features are engineered to decode spatial grayscale data, enabling the characterization of objects or shapes.[39] Transform-based features analyze gray-level patterns in different mathematical spaces through various transformations, including Fourier, Gabor, and Haar wavelet transformation.[35] Artificial intelligence (AI) has demonstrated rapid advancement in medical imaging applications, showing remarkable capabilities in Image segmentation;[40–42] Feature extraction;[31,43] Feature selection and optimization;[44–46] Predictive model development.[47–49] Machine learning (ML), a branch of artificial intelligence, emerges as a promising auxiliary tool.[50] It specializes in identifying the intricate relationships between high-dimensional input radiomics features and target variables, utilizing training examples to develop predictive models with the utmost accuracy.[51] Four commonly used ML methods: reinforcement learning, supervised learning, unsupervised learning, semi-supervised learning, can be used to solve different tasks. In practical applications, common ML methods include support vector machine (SVM), random forest (RF), decision tree (DT) and others. Three common terms in the application of ML are training set, validation set, and test set. The training set is used for model training, the validation set for optimizing hyperparameters, and the test set for evaluating the model's generalization ability. Model performance is often assessed using the receiver operating characteristic (ROC) curve and its area under the curve (AUC). Deep learning (DL), a pivotal subset of ML,[52] forms the foundation of modern AI systems. It harnesses intricate structures or multiple layers of processing—composed of a series of nonlinear transformations—to discern data algorithms and delve into the inherent patterns and representational depths of sample data.[53] Convolutional neural network (CNN) are the most commonly used method in DL. Recent advances demonstrate that ML approaches, particularly DL techniques combined with 18F-FDG PET/CT radiomic features, provide valuable decision-support capabilities for managing patients. Figure 2 depicts the workflow of AI in lymphoma management.

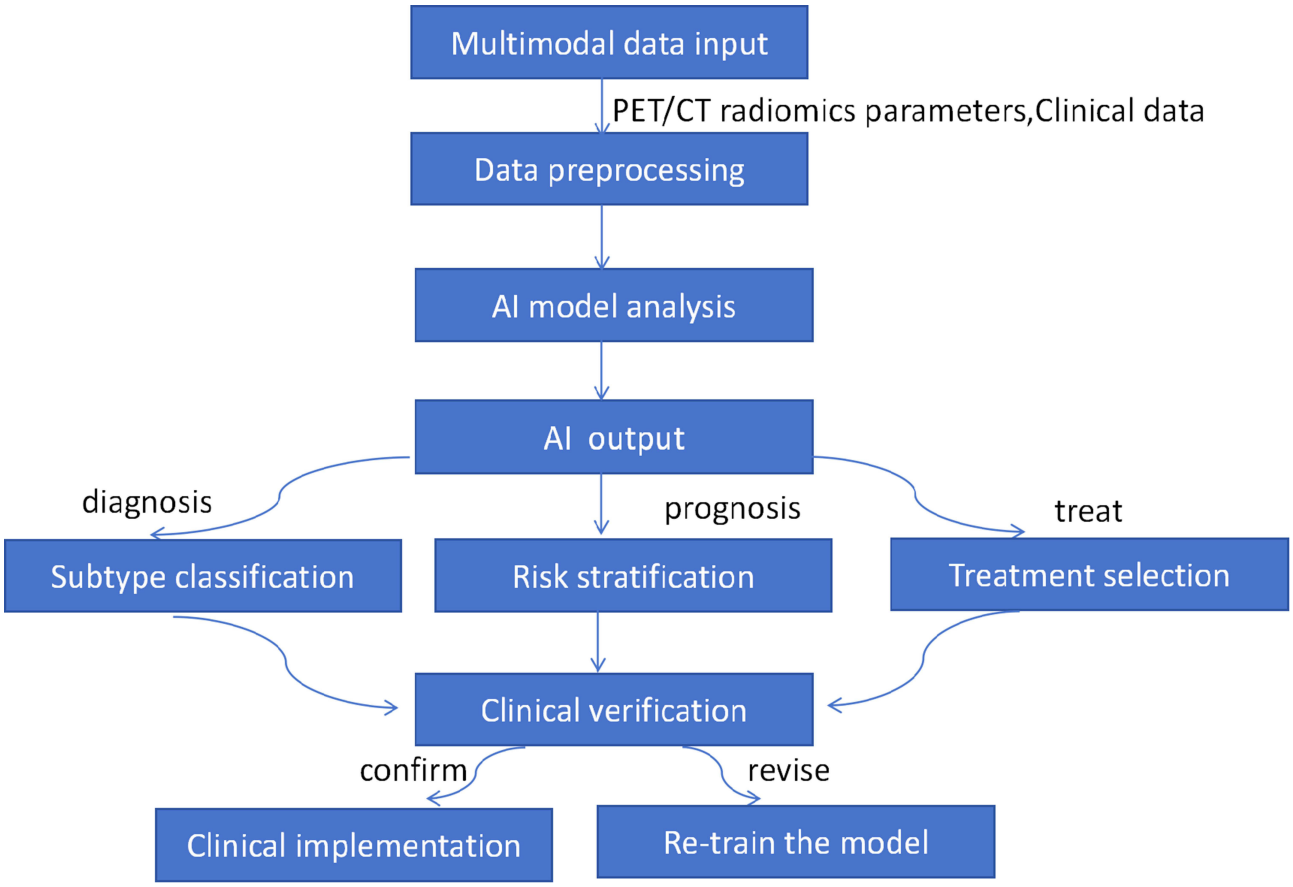

Figure 2 The picture depicts the workflow of AI in lymphoma management.

https://doi.org/10.2147/CMAR.S529589

Recent Innovations in Radiomics for Lymphoma Diagnosis, and Differential Diagnosis

Achieving effective management and accurate prognosis of lymphoma depends fundamentally on timely and early diagnosis.[54,55] Over the past decades, PET/CT radiomics have improved the accuracy of lymphoma diagnosis. The impact of PET/CT radiomics on lymphoma diagnosis has dramatically expanded, evolving from the examination of isolated features to a comparative analysis of models and the employment of advanced deep learning methodologies. Kong et al[56] investigated the utilization of shape, first-order, and texture features derived from 18F-FDG-PET imaging to distinguish central nervous system lymphoma from glioblastoma (GBM). They pinpointed 13 radiomics features capable of effectively discerning lymphoma from GBM, suggesting that lymphoma generally displays higher SUV values across most interval segments and is quantitatively more heterogeneous compared to GBM. This study demonstrated that radiomics features can effectively distinguish GBM from central nervous system lymphoma (Table 1). A retrospective study evaluated the ability of 18F-FDG PET/CT radiomics combined with machine learning to distinguish breast cancer from breast lymphoma.[57] Six unique classification models were created, each containing a distinct combination of clinical and imaging data. The findings indicated that both the PETa model (which merges clinical details with SUV measurements and radiomic features) and CTa model (which combines clinical information and radiomic features derived

Table 1 Application of 18F-FDG PET/CT Radiomic Features in Lymphoma: Diagnosis, Subtyping, Staging, and Risk Stratification

Authors, Year	Patients Number	Clinical Purpose	PET/CT Parameters	Area Under the Curve (AUC Values)
Kong et al 2019[56]	77 patients (24 with lymphoma and 53 with Glioblastoma)	Differential diagnosis between primary central nervous system lymphoma and glioblastoma	Shape, first-order and texture features	0.943–0.998
Ou et al 2020[57]	44 patients (19 with breast lymphoma and 25 with breast cancer)	Differential diagnosis between breast lymphoma and breast cancer	Clinical, SUV, Radiomic features	Training group: 0.867 Validation group: 0.806
Sibille et al 2020[58]	629 patients (327 with lymphoma and 302 with lung cancer)	Differential diagnosis between Lymphoma and lung cancer	Deep Convolutional Neural Networks	0.98
Cui et al 2023[59]	51 patients (8 with PCNSL and 43 with brain metastases)	Differential diagnosis between Primary central nervous system lymphoma (PCNSL) and brain metastases	Density features and the group of multi-class features	0.93
Wang et al 2024[60]	86 patients (69 with pancreatic carcinoma and 17 with pancreatic lymphoma)	Differential diagnosis between pancreatic lymphoma and pancreatic carcinoma	PET metabolic parameters and radiomics features	Training set: 0.994–0.989 Validation set: 0.844–0.909
Zhu et al 2021[61]	38 patients (18 with renal cell carcinoma and 20 with renal lymphoma)	Differential diagnosis between renal lymphoma and renal cell carcinoma	Synthetic texture parameters	0.725–1.0
Lovinfosse et al 2022[62]	420 patients (169 with sarcoidosis, 140 with HL, and 111 with DLBCL)	Lymphoma subtypes classification	Tumor-liver radiomics (TLR)	TLR: 0.95
Mayerhoefer et al 2020[63]	97 patients with MCL	Bone marrow infiltration	SUVmax, SUVmean, SUVpeak, and 16 co-occurring matrix texture features	The radiomic signature: 0.73
Eertink et al 2022[64]	317 patients with DLBCL	Risk stratification	Radiomics(MTV, SUVpeak, and Dmaxbulk) and clinical features	0.79
Ortega et al 2023[65]	88 patients with HL	Risk stratification	65 radiomic features	0.79

from CT scans) exhibited exceptional proficiency in distinguishing between the training and validation groups. Notably, the PETa model achieved an AUC of 0.867 for the training set and 0.806 for the validation set, whereas the CTa model achieved an AUC of 0.891 for the training set and 0.759 for the validation set, showcasing their respective discriminative strengths (Table 1). In a large-scale retrospective case study,[58] 629 patients were enrolled to undergo 18F-FDG PET/CT uptake classification utilizing a deep convolutional neural network (CNN) to discriminate between lymphoma and lung cancer. In the evaluation of CNN performance for 18F-FDG PET/CT imaging, utilizing five input features, distinct results emerged. 18F-FDG PET alone achieved a remarkable AUC of 0.97, highlighting its superior performance. The incorporation of 18F-FDG PET and CT, further enhanced the diagnostic capability with an AUC of 0.98 (Table 1). Significant to highlight that PET/CT radiomics also plays a crucial role in: discerning lymphoma from metastatic tumors;[59] differentiating renal lymphoma from renal cell carcinoma;[60] and distinguishing pancreatic cancer from pancreatic lymphoma (Table 1).[61]

Distinguishing Between the Lymphoma Subtypes

The significant variations in therapeutic interventions and predicted outcomes for individual lymphoma subtypes emphasize the importance of timely pathological subtype classification to guide accurate and tailored treatment plans. Notably, lymphoma subtype and patient heterogeneity are major drivers of patient outcome.[66] At present, lymphoma classification relies on invasive biopsy and pathological analysis. Consequently, the utilization of noninvasive techniques for the automated classification of lymphoma subtypes holds significant clinical implications. An increasing number of studies demonstrate that PET/CT radiomics plays a pivotal role in distinguishing among diverse lymphoma subtypes. Abenavoli EM et al conducted a retrospective review of histopathological diagnoses for mediastinal volume disease. The application of machine learning approaches was utilized to assess the diagnostic importance of 18F-FDG PET/CT volumetric and textural features for identifying distinct histological subtypes of lymphoma. The findings revealed substantial variations in SUV max, SUV mean, MTV, TLG, and various texture features at both first- and second-order gray levels across the lymphoma groups. Among machine learning classifiers, tree-based ensemble techniques demonstrated the highest efficacy for distinguishing lymphoma histological subtypes.[67] Researchers classified patients into four major lymphoma subtypes: DLBCL, FL, HL, and MCL. By integrating multiple-instance learning with support vector machines (SVMs) and random forest classifiers, they achieved 97.0% sensitivity and 94.1% positive predictive value for HL diagnosis, evaluated at both volume-of-interest (VOI) and patient levels.[68] Lovinfosse et al integrated clinical data, including age, sex, and weight, with radiomic features from both original images and tumor-liver radiomics (TLR). They employed seven distinct feature selection methods with four machine learning (ML) classifiers to differentiate HL and DLBCL. The TLR lesion-based approach achieved an AUC of 0.95, while the patient-based approach (incorporating original radiomics and age) yielded an AUC of 0.86 (Table 1).[62] Regarding lymphoma subtype classification, PET/CT radiomics has undertaken multiple endeavors. These endeavors consist of the application of the Radiomics-Deep Learning (RA-DL) approach for tumor subtype classification;[69] as well as the implementation of classification methods that are derived from pseudo-spatiotemporal (PST) radiomics features, and the utilization of structural recurrent convolutional neural networks for distinguishing different subtypes.[70]

One challenge in treating lymphoma is accurately identifying cases that have undergone histological transformation (HT). HT refers to the process whereby indolent lymphoma transforms into a clinically aggressive form. Despite declining conversion rates, the disease remains a substantial threat with poor prognosis.[71–73] Richter transformation (RT), initially delineated by pathologist Moritz Richter in 1928,[74] describes the conversion of chronic lymphocytic leukemia/small lymphocytic lymphoma (CLL/SLL) into aggressive B-cell lymphoma or HL.[75,76] This transformation occurs in roughly 2–10% of cases.[74] Several genetic, clinical, and biological factors are linked to elevated RT risk, yet a unified consensus remains elusive.[77–79] Prognosis is generally poor limited effective treatments.[80–82] Previous studies indicate 18F-FDG can identify transformation from indolent to aggressive lymphoma.[83–85] Among semi-quantitative studies, SUV max has been the most extensively researched.[86–88] A meta-analysis of 1,593 CLL patients established an optimal SUV max threshold of 5 for detecting RT, demonstrating 86.8% sensitivity and 90.5% negative predictive value.[89] In addition to SUV max, studies also incorporated other semi-quantitative parameters. Significant differences between RT and non-RT patients were observed in PET metrics including: maximum standardized uptake value body weight (SUV bw), lean body mass (SUV lbm), body surface area (SUV bsa), lesion-to-liver SUV ratio (L-L SUVR),

and lesion-to-blood-pool SUV ratio (L-BP SUVR).[87,90] Large-cell transformation represents another common form of HT. The predictive value of SUV max for identifying large-cell transformation remains controversial. Previous smaller series suggested an association between baseline SUV max and HT,[91,92] FDG activity was overall higher in HT patients than in histological untransformed patients.[93,94] Nonetheless, some research endeavors have revealed that SUV max does not function as a reliable indicator for predicting HT.[95]

Staging, Especially in the Bone Marrow Infiltration (BMI)

Accurate staging plays a crucial role in devising effective therapeutic strategies for both HL and NHL. According to the National Comprehensive Cancer Network Working Center (NCCN) and Society of Nuclear Medicine (SNM), FDG-PET/CT is indispensable for lymphoma staging.[96] PET/CT implementation has markedly enhanced identification of nodal and extranodal manifestations, allowing for either an upgrade or downgrade in staging.[97–99] Research has indicated that it alters the staging in 18% to 45% of FL patients, 3% to 45% of HL patients, and around approximately 5% of DLBCL diagnoses.[100–104] Bone marrow involvement (BMI) occurs in approximately 50% of patients with NHL and can be seen in up to 15% of HL.[105–107] While bone marrow biopsy (BMB) remains the gold standard for assessing marrow aggressiveness, its reliance on random sampling contributes to high false-negative rates.[108,109] Whether 18F-FDG PET/CT radiomics can replace BMB is a current research focus. The outcomes of numerous visual18F-FDG-PET investigations evaluating bone marrow infiltration proved unsatisfactory, exhibiting either low sensitivity or specificity, particularly with a sensitivity ranging from 12% to 52% in MCL cases.[110–113] Numerous studies have attempted to differentiate involved and uninvolved bone marrow using quantitative PET/CT metrics, yet the findings remain contentious.[89,114–116] Researchers sought to pinpoint threshold values capable of distinctly separating the SUV max, SUV mean, and SUV peak of affected and unaffected bone marrow. They arrived at the optimal cutoff points for cSUV mean (3D partial volume corrected mean standardized uptake value), SUV max, and SUV peak as 1.3, 2.1, and 1.7, correspondingly, resulting in unique pairings of sensitivity and specificity 75.0% and 85.7%, 87.5% and 85.7%, and 87.5% and 85.7%, separately.[116] However, Adams HJ et al included 40 newly diagnosed DLBCL patients in their study and conducted a head-to-head comparison against BMB, revealing a substantial intersection in the cSUV mean, SUV max, and SUV peak values between the groups.[117] Aide and colleagues extracted a range of features from PET scans of 82 DLBCL patients, including histogram, co-occurrence matrix, and size region matrix features. Among the histogram features, SkewnessH was identified as the most accurate measure for determining BMI, with a sensitivity of 81.8% and a specificity of 81.7%.[118] Other studies have incorporated texture analysis and radiomics alongside standard PET parameters. The analysis identified two specific radiomic metrics—code similarity and long-run emphasis—as having significant predictive value for BMI identification.[119] In a separate retrospective study, researchers extracted standard uptake value parameters (SUVmax, SUVmean, SUVpeak) and 16 co-occurring matrix texture features. Utilizing a multilayer perceptron neural network, compared three distinct combinations to predict BMI. SUVs, the radiomic features, and the radiomic features when integrated with laboratory data, showed AUCs reaching up to 0.66, 0.73, and 0.81 for the assessment of involved versus uninvolved bone marrow. These results indicate that FDG-PET texture features augment the predictive power of SUV-based methods for identifying BMI in MCL (Table 1).[63] Therefore, PET/CT-based radiomics plays a pivotal role in precise lymphoma staging and significantly contributes to clinical decision-making.

Treatment Options Based on Risk Stratification

PET/CT radiomics plays a crucial role in personalized lymphoma treatment management. Risk-adapted treatment strategies are essential for optimizing cure rates while minimizing treatment-related toxicity. PET/CT radiomics provides clinically significant quantitative data, facilitating both pretreatment risk stratification and treatment response monitoring through phenotypic characterization. The capacity to identify patients at elevated relapse risk before treatment enables early stratification and potentially improves outcomes.

For the most common type of NHL, DLBCL, current prognostic systems include the International Prognostic Index (IPI),[120] the revised IPI,[121] or the National Comprehensive Cancer Network IPI,[122] do not effectively discern patients at high risk.[123,124] Consequently, recent studies have shown growing interest in using PET/CT-derived biomarkers for initial risk stratification in lymphoma patients to optimize treatment outcomes. Researchers analyzed 152 DLBCL patients, extracting 1245 radiomics features from pretreatment PET/CT images, with primary focus on total metabolic tumor volume (TMTV) and metabolic tumor volume (MTV). These features, alongside clinical variables, were employed to develop a mixed nomogram. The AUC values for

TMTV and MTV were significantly higher than those of the IPI. Decision curve analysis (DCA) demonstrated that the composite nomogram provided greater net benefit than the IPI alone. By integrating RF and IPI, the nomogram incorporating MTV and TMTV achieved more pronounced risk stratification compared to IPI alone, with more significant differences among subgroups and an enhanced risk ratio.[125] 95 individuals with advanced DLBCL were included in the study. Baseline MTV and radiomics features were calculated. Patients exhibiting elevated MTV and Dmax (maximum tumor dissemination) were identified as having risk factors for reduced progression-free survival (PFS). Furthermore, these factors correlated with reduced overall survival (OS). Combining MTV (> 384 cm^3) and Dmax (> 58 cm) established three distinct risk categories. They suggest that integrating MTV with parameters reflecting tumor burden spread improves DLBCL staging risk stratification.[126] A model integrating metabolic heterogeneity (MH) with MTV can early identify patients with refractory DLBCL who could benefit from intensive therapy. High-risk patients with a diminished PFS (HR=5.6) and shortened OS (HR=7.6).[127] To identify DLBCL patients at high risk of disease progression or relapse, baseline lesions were delineated using semi-automated segmentation (SUV≥4.0) and 490 radiomics features were extracted.[64] The fusion of radiomics and clinical features, particularly the blend of tumor-centric indicators (MTV, SUV peak, and D maxbulk) with patient-centric parameters (WHO performance status and age exceeding 60 years), yielded the highest performance with an AUC of 0.79 (Table 1). The incorporation of radiomics features into clinical features resulted in a 15% elevation in PPV (positive predictive value), thereby increasing the exactness in pinpointing high-risk patients.

Most HL patients have a favorable prognosis.[128,129] However, early identification of the minority with refractory or recurrent disease, which can be life-threatening, would be clinically invaluable.[130,131] A retrospective analysis of 267 stage I–II HL patients found that in multivariate Cox regression, a 100-unit increase in total MTVt (HR = 1.14) and a 500-unit increase in total TLGt (HR = 1.096) significantly correlated with freedom from progression. This suggests MTV and TLG provide quantifiable tumor burden indicators for HL risk stratification.[132] In order to precisely detect patients who are at a high risk for HL, the authors incorporated a cohort consisting of 258 patients diagnosed with stage I to II, who had undergone baseline PET scans and interim PET scans (iPET 2) following the completion of two treatment sessions (doxycycline, bleomycin, vinblastine, and dacarbazine).[133] Four high-risk categories were defined by TMTV (with a threshold of 147) and interim PET 2 (DS score), displaying a 5-year PFS of 95%, 81.6%, 50% and 25%, respectively. Compared to existing staging frameworks (EORTC,[134] GHSG,[135] NCCN)[136], TMTV improves initial risk assessment, enabling earlier treatment intensification and timelier therapeutic decisions.[137,138] For predicting HL radiotherapy need, 65 radiomics features and clinical parameters were analyzed using binary logistic regression to identify predictors and calculate odds ratios (OR).[65] The findings revealed that the first-order PET parameter sphericity (OR = 1.9), the CT parameter gray level zone length matrix high gray level zone emphasis (GLZLM SZHGE mean, OR = 2), PARAMS spatial resampling (OR = 2.1), and abnormal hemoglobin levels served as predictors for the final model, which achieved an AUC of 0.79 (Table 1).

Predicting Prognosis

Studies have identified multiple prognostic factors associated with lymphoma outcomes. IPI is regarded as a prognostic framework that is grounded in the characteristics of various clinical factors, encompassing age, Ann Arbor stage, extranodal involvement, serum lactate dehydrogenase (LDH) levels, and performance status.[120] However, these conventional parameters primarily function as indirect proxies for tumor burden and fail to fully capture functional and metabolic tumor characteristics.[139,140] Recent advances in PET/CT imaging have revealed various quantitative biomarkers with potential prognostic value. These indicators encompass a spectrum from semi-quantitative metrics to tumor volume, and extend to metabolic characteristics (eg, shape and texture).

SUV Indicators Used for Predicting Outcomes

Owing to its stability and reproducibility, SUV max is the most widely used parameter in lymphoma prognostic studies. Multiple studies have demonstrated correlations between SUV max and survival outcomes in lymphoma patients.[141–145] Researchers have proposed SUV max as a key predictor of disease progression in DLBCL. Using a cutoff value of 15, they found that patients with SUV max <15 had a 3-year overall survival (OS) of 90%, while those with SUV max ≥15 showed 72% survival. PFS was 90% for the low SUV max group and 39% for the high SUV max group.[141] A retrospective analysis included 123 elderly patients with HL who underwent baseline18F-FDG-PET/CT scans at the onset of treatment and subsequent PET/CT scans at the conclusion of therapy. Through semi-quantitative index analysis, they explored whether baseline PET/CT metabolic parameters could be used

as prognostic indicators for HL. The results showed that both L-BP SUVR (lesion to blood-pool SUV max ratio) and L-L SUV R (lesion to liver SUV max ratio) were significantly associated with PFS and OS.[143] In patients diagnosed with extranodal natural killer/T-cell lymphoma (NKTCL), a baseline SUV max of 9.65 emerged as an independent predictor of poor prognosis for distant relapse-free survival (HR=4.58) and PFS (HR=2.6). The authors suggest that the baseline SUV max could be a useful tool for identifying NKTCL patients at heightened risk of disease progression.[146] Nevertheless, some studies indicate that the prognostic predictive ability of SUV max in lymphoma is limited. One large-scale study indicated that SUV max has negligible predictive value for PFS and OS in 258 patients with stage I and II HL.[133]

SUV max represents the most widely studied PET/CT biomarker in lymphoma prognosis, though its prognostic reliability remains debated. This ambiguity may stem from various factors influencing the SUV, including the spatial resolution of the scanner, the image acquisition protocols, and the PET reconstruction parameters. Furthermore, clinical study limitations such as heterogeneous cohort sizes across disease stages, along with differences in therapeutic regimens and progression-free survival (PFS) criteria, collectively contribute to the persistent uncertainty regarding its prognostic utility.[147,148]

Tumor Burden Metrics for Prognostic Prediction

While SUV max primarily characterizes the most metabolically active tumor regions, it does not fully capture spatial heterogeneity within the lesion. Moreover, it overlooks critical prognostic elements, particularly tumor burden information. Recently, innovative metrics reflecting aggregate tumor burden, such as MTV and TLG, have been employed to predict PFS and OS in lymphoma patients. These indicators have been identified as potential baseline predictors for prognosis in different types of lymphoma.[149–151]

The determination of the SUV threshold plays a pivotal role in delineating the boundary of lymphoma lesions, which in turn influences the calculation of the MTV. Commonly used thresholds include 41% of SUV max,[152,153] SUV 4,[154,155] and SUV max set at 2.5,[156] among others. As depicted in Figure 3, the contour range varies for an example DLBCL patient at different thresholds. To a certain degree, the diverse cut-offs utilized could have played a role in the survival

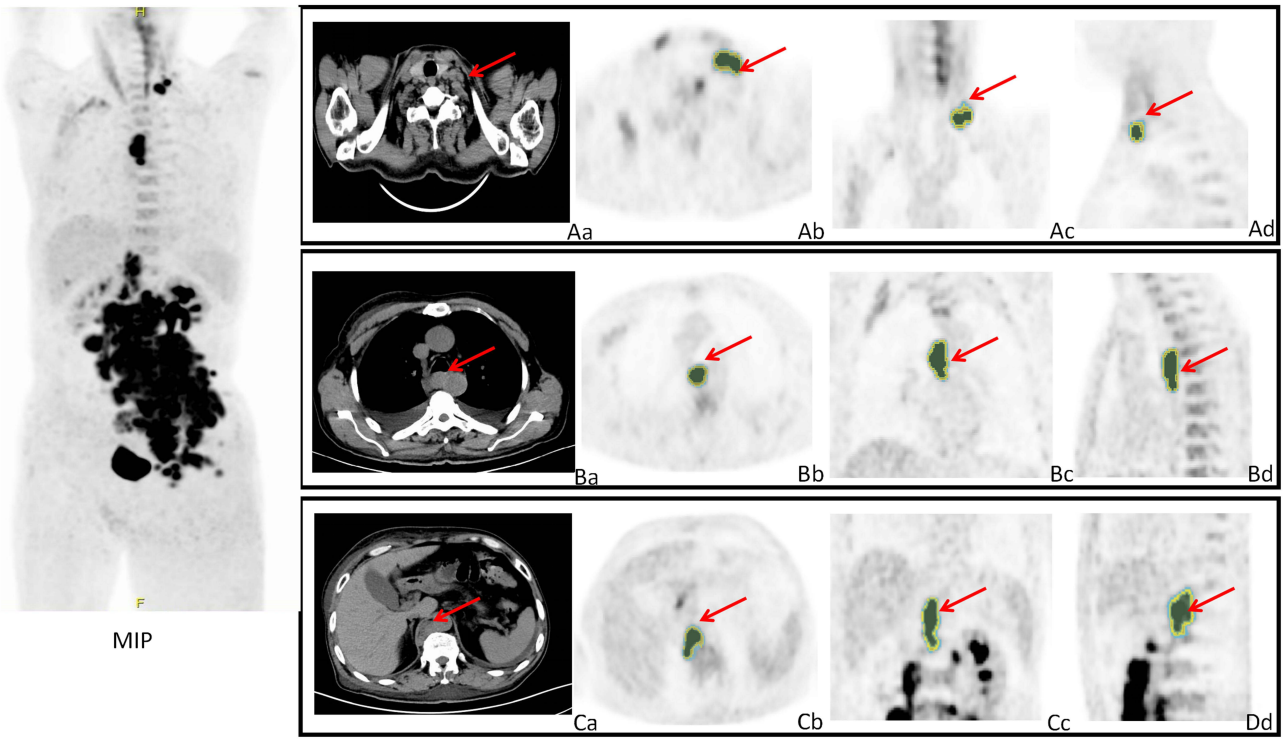

Figure 3 FDG PET/CT images in a DLBCL patient show three distinct contouring thresholds (red arrows): Green= 41% SUV max; Yellow= 2.5 SUV; Blue= 1.5× liver SUV mean (3D Slicer [https://www.slicer.org/]). (A(a–d)) Left supraclavicular lymph node; (B(a–d)) Mediastinal lymph node; (**C**a–d) Retroperitoneal lymph node ((**A**) axial CT (**B**) axial PET; (**C**) coronal PET; (**D**) sagittal PET).
Abbreviation: MIP, Maximum intensity projection.

differences observed between the groups. Determining the suitable SUV threshold for MTV computation is dependent on the specific patient cohort under evaluation.

Researchers conducted a retrospective analysis of 169 patients with stage II–III DLBCL. The boundary of the target lesion was delineated employing a SUV threshold of 2.5, and MTV was subsequently quantified. ROC analysis identified 220 cm^3 as the optimal MTV cutoff value. Patients with a lower MTV (<220 cm^3) demonstrated significantly prolonged PFS and OS in comparison to those with a higher MTV (≥220 cm^3)[157] (Table 2). In another study, margin values were determined using lesion SUV max thresholds of 25%, 50%, and 75%, which correspondingly yielded TLG values of TLG25, TLG50, and TLG75. High TLG50 values (> 415.5) were linked to decreased survival rates in comparison to low TLG 50 values (≤415.5) (73% versus 92% for 2-year PFS; 2-year OS 81% versus 93%). A high IPI score significantly diminished the OS (2-year OS: 79% vs 90%). Ann Arbor Phase III/IV had an adverse effect on the PFS (P=0.013). However, neither higher IPI scores nor stage III/V alone significantly impacted PFS. High TLG50 values independently predicted survival outcomes, with hazard ratios (HR) of 4.4 for

Table 2 Summary of Included Prognostic Studies by Lymphoma Type

Type		Authors	Patients Number	Study Type	Multi-Centre	Treatment	Features	Definition of Prognostic Factor Provide	Median Follow-Up Time
NHL	DLBCL	Song et al[157]	169	Retrospective study	No	R-CHOP	MTV	PFS OS	36 months
	DLBCL	Kim et al[158]	140	Retrospective study	No	R-CHOP	SUVmax TLG	2-year PFS OS	28.5 months
	DLBCL	Kostakoglu et al[160]	1418	Retrospective study	Yes	R-CHOP	TMTV, TLG,	OS PFS	48 months
	DLBCL	Capobianco et al[163]	301	Retrospective study	Yes	R-CHOP	TMTVPARS TMTVREF	PFS OS	5 years
	FL	Meignan et al[167]	185	Retrospective study	Yes	R-CHOP R-CVP R-FM	TMTV	5-year PFS OS	64 months
	DLBCL	Cottereau et al[170]	290	Retrospective study	Yes	R-CHOP	D max SD max MTV	4-year PFS OS	5 years
	DLBCL	Cottereau et al[126]	95	Retrospective study	Yes	R-CHOP R-ACVBP	MTV Dmax	4-year PFS OS	44 months
	Mediastinal B-cell lymphoma	Ceriani et al[171]	103	Clinical trial	Yes	R-CHOP R-CHOP-like	MH TLG MTV	5-year PFS	62 months
	DLBCL	Ceriani et al[127]	254	Retrospective study	Yes	R-CHOP	MTV MH	5-year PFS OS	Testing set: 64 months Validation set: 36 months
	DLBCL	Aide et al[172]	132	Retrospective study	No	R-CHOP R-ACVBP	MTV Radiomic features	2y-EFS	27 months
	DLBCL	Ritter et al[173]	85	Retrospective study	Yes	R-CHOP	Radiomic features	2y- EFS	/
	DLBCL	Frood et al[174]	229	Retrospective study	No	R-CHOP	Radiomic features	2-EFS	/
HL	HL	Kanoun et al[159]	59	Retrospective study	No	Chemotherapy	TMTV	4-year PFS	50 months
	cHL	Voorhees et al[166]	27	Clinical trial	No	CD30.CAR-T	MTV	PFS	9.5 months
	HL	Gallamini et al[175]	783	Clinical trial	Yes	ABVD	D max TMTV	3-year PFS	40.6 months
	cHL	Frood et al[176]	289	Retrospective study	No	ABVD AVD	Radiomic features	2-EFS	/
	HL	Milgrom et al[177]	251	Retrospective study	No	ABVD	MTV TLG Radiomic features	/	/

https://doi.org/10.2147/CMAR.S529589

PFS and 3.1 for OS[158] (Table 2). To assess baseline metabolic tumor volume (TMTV 0) in HL patients, TMTV 0 was quantified was quantified using a semi-automated technique with an SUVmax threshold of 41%. Both TMTV0 (225mL) and tumor volume (10 cm) were found to be indicators of PFS at the 4-year mark, with survival rates of 42% versus 85% and 44% versus 79%, respectively. Multivariate analysis confirmed TMTV0 (relative risk [RR] = 4.4) as an independent PFS predictor, demonstrating stronger prognostic value than tumor volume in HL patients[159] (Table 2). Investigator findings from Phase III of the GOYA study indicated that elevated TMTV (366cm³) and TLG (3004g) were associated with inferior PFS in patients with DLBCL[160] (Table 2). This study is based on the III GOYA study, and the prospective, standardized PET procedure and a large number of PET-CT scan samples at baseline enhance the confidence in the data conclusions and further confirm the prognostic value of baseline quantitative PET indicators in lymphoma. To date, no consensus exists on standard techniques for contouring MTV and TLG, despite numerous proposed limitations to define metabolically active tumors.[158,161,162] In PET/CT scans of 301 DLBCL patients, three-dimensional (3D) regions of interest (ROIs) were identified using an automated whole-body high-uptake segmentation algorithm and processed with a convolutional neural network (CNN) to calculate TMTVPARS. These results were compared with TMTVREF (measured by two experienced experts utilizing independent semi-automated software). The analysis showed strong agreement between TMTVPARS and TMTVREF, with both demonstrating significant predictive value for PFS and OS in DLBCL patients[163] (Table 2). In relapsed/refractory (R/R) cHL, high MTV at relapse and prior to AutoSCT (Autologous Stem Cell Transplantation) predicted more severe PFS.[164,165] Researchers are developing CD30-targeted chimeric antigen receptor T (CAR-T) cells for R/R HL treatment. Preliminary results from patients treated with CAR T cells suggest that high MTV (60mL) before lymphocyte depletion is associated with PFS at one year. The 1-year PFS rates were 14% versus 58% for high and low MTV groups, respectively[166] (Table 2). Similar to DLBCL and HL, MTV independently predicts outcomes in FL patients[167,168] (Table 2). In 185 FL patients receiving chemoimmunotherapy, the optimal MTV cutoff was 510 cm³. Patients with elevated MTV had significantly reduced survival rates (5-year PFS: 33%, HR=2.90; 5-year OS: 85%, HR=3.45).[167] A meta-analysis of 27 studies demonstrated MTV's prognostic value, with a pooled HR of 3.05 for PFS.[169] In summary, MTV and TLG cut-off values were customized for particular patient groups, and the SUV thresholds applied require careful consideration when contrasting findings from distinct studies.

Parameters That Quantify Tumor Spread Predict Prognosis

Although metabolic tumor volume (MTV) provides volumetric assessment, it fails to account for the spatial complexity of multifocal lymphoma manifestations. Typically, lymphoma involves numerous scattered nodal areas that can be connected to sites outside the nodes, often resulting in mutation-related heterogeneity that influences clinical outcome.[126] Maximum tumor dissemination (D max) serves as a novel radiological indicator, representing the maximum distance between the two farthest lesions.[178] Some studies have employed standardized D max (SD max), which adjusts the peak dose according to body surface area.[170,179] This geometric parameter offers unique advantages: (1) Simplified computation requiring minimal contour dependency; (2) Enhanced reproducibility across imaging platforms and operators; (3) Strong prognostic correlation in lymphoid malignancies. Clinical validation studies confirm Dmax's independent predictive value for PFS and OS in both HL and DLBCL[170,175] (Table 2). In HL patients treated with ABVD, Dmax correlated with 3-year PFS. The most precise threshold for forecasting treatment outcomes was determined to be 16.2cm, with an AUC of 0.62[175] (Table 2). Another retrospective study found Dmax significantly predicted PFS (HR=4.3) and OS (HR=3.7) in advanced HL[126] (Table 2).

Parameters of Metabolic Heterogeneity in Predicting Prognosis

Metabolic heterogeneity (MH) serves as a marker for the diverse patterns of 18F-FDG uptake seen in tumors, distinct from the traditional evaluation of tumor volume and structure. MH encompasses a complex set of factors—including cellular metabolism, growth kinetics, vascular dynamics, and oxygen deprivation—that collectively capture the clinical and molecular complexities of the disease. MH quantification in the dominant lesion (largest MTV) employed the area under the cumulative SUV—volume histogram (AUC-CSH) curve[180]—a method well-documented in solid tumors and lymphoid malignancies.[181–183] A prospective study of 103 primary mediastinal B-cell lymphoma (PMBCL) patients found no significant correlation between MH values and other baseline quantitative PET parameters (SUV max, MTV, and TLG), regardless of methodology. In the stepwise Cox model, elevated MH (HR=12.8) independently predicted

substantially reduced PFS[171] (Table 2). Similarly, among DLBCL patients receiving standard immunotherapy (R-CHOP regimen), elevated MH predicted a significantly worse prognosis in the patient group with higher MTV[127] (Table 2).

Structural and Texture Analysis Predicts the Prognosis

Radiomics enables high-throughput extraction of quantitative imaging features through computational analysis of subvisual patterns in medical imaging data.[184] In DLBCL prognosis research, the study demonstrated that integrated assessment of MTV with second-order texture parameters (homogeneity, contrast, correlation, dissimilarity) and higher-order features (LZE, LZLGE, LZHGE, GLNU, ZP) significantly predicts 2-year event-free survival (2y-EFS). Multivariate analysis identified LZHGE as an independent prognostic marker (HR=7.47)[172] (Table 2). Researchers conducted a retrospective analysis of PET/CT-derived radiomic features and clinical parameters to predict 2y-EFS in DLBCL patients. The analysis identified five key predictors: Maximum diameter, NGTDM busyness, TLG, TMTV, and NGTDM coarseness[173] (Table 2). Another study analyzed baseline PET/CT scans from 229 DLBCL patients treated with R-CHOP[174] (Table 2). Logistic regression models incorporating MTV and six machine learning classifiers were trained and optimized using 4-fold cross-validation. The model that achieved the greatest mean validation AUC combined clinical and radiomic features using a ridge regression approach. It achieved a mean training AUC of 0.77±0.02, and a test AUC of 0.73, outperforming the model that utilized MTV features alone, which yielded an AUC of 0.67. These results demonstrate the clinical utility of radiomic-based predictive modeling for DLBCL outcomes.

Similarly, multiple studies have investigated HL. Researchers evaluated PET/CT radiomic parameters in 251 stage I–II HL patients treated at a tertiary cancer center. The model was crafted and validated through a machine learning algorithm, which resulted in an impressive AUC of 95.2% for the five most predictive features. These features include the first-order feature SUV max and volume, as well as the second-order features: information measure Corr 1, information measure Corr 2, and the mean variance derived from GLCM 2.5. These findings suggest PET/CT radiomic features may predict refractory disease in early-stage HL[177] (Table 2). Another study analyzed 289 cHL patients. The PET/CT data were segmented employing 1.5 × mean liver SUV and a fixed SUV threshold of 4.0, while radiomics features were derived employing PyRadiomics with ComBat harmonization. The ridge regression model (1.5 × mean liver SUV segmentation) showed optimal performance, with validation AUC of 0.79 ± 0.01. The model incorporated age alongside four radiomic features: PET flatness, the length of the PET major axis, GLSZM, GLCM, and the PET lbp-3D-m2. This study confirms that machine learning models based on pre-treatment FDG PET/CT scans can predict outcomes in cHL patients[176] (Table 2).

In conclusion, SUV max represents the most metabolically active region of the tumor and is characterized by high stability and excellent reproducibility. Although widely used in lymphoma prognostic studies, SUV max has limited predictive value for clinical outcomes. MTV and TLG provide better prognostic assessment by quantifying overall tumor burden and heterogeneity. However, clinical application faces a key challenge: standardization of SUV threshold definitions. Dmax—the interlesional distance between two farthest lesions—shows high reproducibility and promising prognostic value in lymphoma. Unfortunately, in actual clinical practice, Dmax tends to be neglected. Metabolic heterogeneity (MH) reflects complex tumor biology (cellular metabolism, proliferation kinetics, vascularity, and hypoxia) and strongly correlates with lymphoma aggressiveness. Furthermore, the integration of structural and texture analysis with AI has significantly enhanced PET/CT's predictive capability in lymphoma prognosis (Table 3).

Table 3 Application of 18F-FDG PET/CT Radiomic Features in Predicting Lymphoma Prognosis

Parameters	Meaning of Parameter in Lymphoma	Clinical Application Characteristics
SUVmax	Reflects the most active part of the lymphoma	High stability and repeatability
MTV and TLG	Reflects tumor burden information	Strong predictive factors
Maximum tumor dissemination (Dmax)	Reflects the dispersibility of lymphoma lesions	Easy to calculate; a novel imaging features
Metabolic heterogeneity (MH)	Encompasses complex factors such as cell metabolism, growth kinetics, vascular dynamics, and hypoxia	Related to invasive biology
Structural, Texture analysis	Radiomic features	Significantly enhanced the predictive capability

https://doi.org/10.2147/CMAR.S529589

The application of AI in PET/CT clinical trials for lymphoma has significantly enhanced diagnostic accuracy and treatment efficacy assessment efficiency. Deep learning-based automatic lesion segmentation and quantitative analysis have reduced human bias while improving result reproducibility. Research has shown that AI models, when combined with radiomics features, can predict treatment responses and prognoses more accurately and earlier. However, challenges remain regarding multicenter data standardization, algorithm interpretability, and clinical translation pathways. Future research should focus on large-scale prospective validation and developing AI-driven clinical trial designs to advance precision medicine in lymphoma management.

PET/CT Parameters and CAR-T Therapy

In lymphoma treatment, immunotherapy and chemoimmunotherapy have emerged as increasingly prominent therapeutic approaches, complementing conventional chemotherapy. CAR-T cell therapy, also known as chimeric antigen receptor T cell therapy, is a new approach in the field of immunotherapy for NHL. Studies have shown that 18F-FDG PET/CT radiomics parameters play a key role in monitoring treatment response, evaluating the efficacy of immunotherapy, assessing treatment-related toxicity, and predicting prognosis in CAR-T therapy. Baseline SUV max can predict PFS following CAR-T treatment, and the baseline volume parameters (MTV and TLG) are potential prognostic indicators of CAR-T treatment affecting PFS and OS.[185] The two most prevalent adverse effects of CAR-T cell therapy are cytokine release syndrome (CRS) and neurotoxicity. CRS is characterized by a systemic inflammatory response caused by the rapid release of cytokines from activated CAR-T cells, while neurotoxicity manifests as neurological symptoms such as seizures and disorientation. Multiple PET/CT parameters (SUV max, SUV avg, MTV, TLG) may help predict and assess the severity of these toxicities in CAR-T recipients.[186] Thus, 18F-FDG PET/CT parameters offer a comprehensive strategy for managing CAR-T therapy patients, facilitating timely clinical interventions and serving as crucial prognostic tools for lymphoma patients undergoing this treatment.

Limitations and Challenges

Despite the rapid development of PET/CT radiomics in lymphoma, several challenges remain. The primary challenge involves image quality control, as high-quality imaging data constitute a prerequisite for radiomics analyses. One study examined data heterogeneity arising from variations in acquisition parameters, such as scan duration, iteration and subset numbers, reconstruction type and algorithm, and spatial resolution, as well as image processing methodologies, including segmentation techniques and gray level discretization.[176] Among these factors, spatial resolution variations demonstrated the most pronounced impact, with a coefficient of variation reaching 3.63. A series of guidelines and standards have been progressively implemented including the Radiomics Quality Score (RQS), the Image Biomarker Standardization Initiative (IBSI), the AI in Medical Imaging Checklist (CLAIM), and the Quantitative Imaging Biomarkers Alliance (QIBA), among others.[36,187,188] These aim to establish unified imaging protocols and analytical standardization. Second, most current lymphoma radiomics studies adopt retrospective designs. Given lymphoma's heterogeneity and subtype transformation potential, obtaining pathological information from a single or limited sites poses challenges in ensuring that each lesion under investigation has corresponding pathological results. This limitation may introduce selection bias in region-of-interest (ROI) delineation and case inclusion. Consequently, large-scale prospective multicenter studies featuring independent external validation through multi-institutional collaborations are required to enhance clinical data granularity, optimize model robustness, and ensure broad applicability.[51]

Artificial intelligence (AI) has demonstrated versatile applications in medical imaging, including refined attenuation correction, artifact-free image reconstruction, and automated annotation enhancements. As a core component of AI, deep learning has revolutionized medical imaging workflows, powering key tasks such as automated segmentation, multi-modal registration, image fusion, feature engineering, feature extraction, computer-aided diagnosis, and prognostic analysis. These advancements significantly improve the precision and dependability of imaging radiomics classification and predictive analytics. Thus, the incorporation of deep learning into the multifaceted stages of imaging radiomics to offset its inadequacies is expected to shape the forthcoming developmental path for imaging radiomics technology.

In addition, clinicians increasingly aware that single lymphoma biopsy samples inadequately reflect patient genomic profiles. Radiomics can be combined with genomic data (circulating tumor DNA, MYC rearrangement rearrangements)

to provide more accurate biological information for lymphoma patients.[189] This aids in monitoring the progression of lymphoma at the molecular level. Research has revealed a correlation between lymphoma imaging phenotypes and gene expression patterns, which is particularly appealing in the management of lymphoma patients.Thus, the authors hold the belief that the integration of PET/CT imaging, radiomics, and genomic data presents significant potential for exploration and application in the clinical management of lymphoma patients.

While our manuscript demonstrates the significant application value of FDG PET/CT imaging radiomics in the comprehensive management of lymphoma, we acknowledge several limitations. These include, but are not limited to, the lack of: lymphoma subtype-specific classification, qualitative properties analysis, histopathological heterogeneity evaluation, and comprehensive overview of treatment and baseline characteristics as cited in the literature.

Conclusions

By correlating imaging features with the biological, pathological, and metabolic profiles of lymphoma, AI-assisted PET/CT radiomics enhances the clinical differential diagnosis of lymphoma, aids in the early risk stratification and prognostic prediction, and offers a foundation for the formulation of personalized lymphoma treatment strategies. This technology establishes a transformative link between medical imaging and precision oncology, driving the evolution of lymphoma management from macroscopic evaluations to microscopic characterizations, and from empirical approaches to biomarker-driven paradigms. We firmly believe that AI-assisted PET/CT radiomics will make accurate diagnosis and treatment of lymphoma possible in the future.

Acknowledgments

The authors give their thanks to all those who have helped with this issue.

Author Contributions

All authors made a significant contribution to the work reported, whether that is in the conception, study design, execution, acquisition of data, analysis and interpretation, or in all these areas; took part in drafting, revising or critically reviewing the article; gave final approval of the version to be published; have agreed on the journal to which the article has been submitted; and agree to be accountable for all aspects of the work.

Funding

Shandong Province Medical and Health Technology Project (No. 202301060260). Sailing Project, Scientific Research Foundation of Jining No.1 People's Hospital (2024-QHM-005).

Disclosure

The authors declare that the research was conducted in the absence of any commercial or financial relationships that could be construed as a potential conflict of interest.

References

1. Bray F, Laversanne M, Sung H, et al. Global cancer statistics 2022: GLOBOCAN estimates of incidence and mortality worldwide for 36 cancers in 185 countries. *CA Cancer J Clin*. 2024;74(3):229–263. doi:10.3322/caac.21834
2. Shanbhag S, Ambinder RF. Hodgkin lymphoma: a review and update on recent progress. *CA Cancer J Clin*. 2018;68(2):116–132. doi:10.3322/caac.21438
3. Mayerhoefer ME, Umutlu L, Schöder H. Functional imaging using radiomic features in assessment of lymphoma. *Methods*. 2021;188:105–111. doi:10.1016/j.ymeth.2020.06.020
4. Chapuy B, Stewart C, Dunford AJ, et al. Author Correction: molecular subtypes of diffuse large B cell lymphoma are associated with distinct pathogenic mechanisms and outcomes. *Nat Med*. 2018;24(8):1290–1291. doi:10.1038/s41591-018-0097-4
5. Schmitz R, Wright GW, Huang DW, et al. Genetics and Pathogenesis of Diffuse Large B-Cell Lymphoma. *N Engl J Med*. 2018;378(15):1396–1407. doi:10.1056/NEJMoa1801445
6. Gerlinger M, Rowan AJ, Horswell S, et al. Intratumor heterogeneity and branched evolution revealed by multiregion sequencing. *N Engl J Med*. 2012;366(10):883–892. doi:10.1056/NEJMoa1113205
7. Marusyk A, Almendro V, Polyak K. Intra-tumour heterogeneity: a looking glass for cancer? *Nat Rev Cancer*. 2012;12(5):323–334. doi:10.1038/nrc3261

8. Stanta G, Bonin S. Overview on Clinical Relevance of Intra-Tumor Heterogeneity. *Front Med*. 2018;5:85. doi:10.3389/fmed.2018.00085
9. Pribluda A, de la Cruz CC, Jackson EL. Intratumoral Heterogeneity: from Diversity Comes Resistance. *Clin Cancer Res*. 2015;21(13):2916–2923. doi:10.1158/1078-0432.Ccr-14-1213
10. Sohn MH, Kim SI, Shin JY, et al. Classification of High-Grade Serous Ovarian Carcinoma by Epithelial-to-Mesenchymal Transition Signature and Homologous Recombination Repair Genes. *Genes*. 2021;12(7):1103. doi:10.3390/genes12071103
11. Ansell SM. Non-Hodgkin Lymphoma: diagnosis and Treatment. *Mayo Clin Proc*. 2015;90(8):1152–1163. doi:10.1016/j.mayocp.2015.04.025
12. Ansell SM. Hodgkin Lymphoma: diagnosis and Treatment. *Mayo Clin Proc*. 2015;90(11):1574–1583. doi:10.1016/j.mayocp.2015.07.005
13. Cheson BD, Fisher RI, Barrington SF, et al. Recommendations for initial evaluation, staging, and response assessment of Hodgkin and non-Hodgkin lymphoma: the Lugano classification. *J Clin Oncol*. 2014;32(27):3059–3068. doi:10.1200/jco.2013.54.8800
14. Amador-Ortiz C, Chen L, Hassan A, et al. Combined core needle biopsy and fine-needle aspiration with ancillary studies correlate highly with traditional techniques in the diagnosis of nodal-based lymphoma. *Am J Clin Pathol*. 2011;135(4):516–524. doi:10.1309/ajcp3wz8zdrjqdou
15. Frederiksen JK, Sharma M, Casulo C, Burack WR. Systematic review of the effectiveness of fine-needle aspiration and/or core needle biopsy for subclassifying lymphoma. *Arch Pathol Lab Med*. 2015;139(2):245–251. doi:10.5858/arpa.2013-0674-RA
16. Kirienko M, Cozzi L, Rossi A, et al. Ability of FDG PET and CT radiomics features to differentiate between primary and metastatic lung lesions. *Eur J Nucl Med Mol Imaging*. 2018;45(10):1649–1660. doi:10.1007/s00259-018-3987-2
17. Moon SH, Kim J, Joung JG, et al. Correlations between metabolic texture features, genetic heterogeneity, and mutation burden in patients with lung cancer. *Eur J Nucl Med Mol Imaging*. 2019;46(2):446–454. doi:10.1007/s00259-018-4138-5
18. Choi ER, Lee HY, Jeong JY, et al. Quantitative image variables reflect the intratumoral pathologic heterogeneity of lung adenocarcinoma. *Oncotarget*. 2016;7(41):67302–67313. doi:10.18632/oncotarget.11693
19. Nair VS, Gevaert O, Davidzon G, et al. Prognostic PET 18F-FDG uptake imaging features are associated with major oncogenomic alterations in patients with resected non-small cell lung cancer. *Cancer Res*. 2012;72(15):3725–3734. doi:10.1158/0008-5472.Can-11-3943
20. Sala E, Mema E, Himoto Y, et al. Unravelling tumour heterogeneity using next-generation imaging: radiomics, radiogenomics, and habitat imaging. *Clin Radiol*. 2017;72(1):3–10. doi:10.1016/j.crad.2016.09.013
21. Voltin CA, Mettler J, Grosse J, et al. FDG-PET Imaging for Hodgkin and Diffuse Large B-Cell Lymphoma-An Updated Overview. *Cancers*. 2020;12(3):601. doi:10.3390/cancers12030601
22. Khan S, Naim S, Bilwani R, et al. Radiogenomics and Its Role in Lymphoma. *Curr Hematol Malig Rep*. 2020;15(3):211–224. doi:10.1007/s11899-020-00577-2
23. Zhang Y, Deng Y, Zou Q, et al. Artificial intelligence for diagnosis and prognosis prediction of natural killer/T cell lymphoma using magnetic resonance imaging. *Cell Rep Med*. 2024;5(5):101551. doi:10.1016/j.xcrm.2024.101551
24. Zhang X, Zhao Z, Wang R, et al. A multicenter proof-of-concept study on deep learning-based intraoperative discrimination of primary central nervous system lymphoma. *Nat Commun*. 2024;15(1):3768. doi:10.1038/s41467-024-48171-x
25. Sakamoto K, Uchiyama K, Iwasaki T, Inaba H, Matsuura K. An artificial viral capsid decorated with a DNA aptamer internalizing into lymphoma cells. *J Mater Chem B*. 2023;11(26):6053–6059. doi:10.1039/d3tb00169e
26. Rizzo S, Botta F, Raimondi S, et al. Radiomics: the facts and the challenges of image analysis. *Eur Radiol Exp*. 2018;2(1):36. doi:10.1186/s41747-018-0068-z
27. Lucia F, Visvikis D, Vallières M, et al. External validation of a combined PET and MRI radiomics model for prediction of recurrence in cervical cancer patients treated with chemoradiotherapy. *Eur J Nucl Med Mol Imaging*. 2019;46(4):864–877. doi:10.1007/s00259-018-4231-9
28. Mayerhoefer ME, Riedl CC, Kumar A, et al. Radiomic features of glucose metabolism enable prediction of outcome in mantle cell lymphoma. *Eur J Nucl Med Mol Imaging*. 2019;46(13):2760–2769. doi:10.1007/s00259-019-04420-6
29. Lambin P, Rios-Velazquez E, Leijenaar R, et al. Radiomics: extracting more information from medical images using advanced feature analysis. *Eur J Cancer*. 2012;48(4):441–446. doi:10.1016/j.ejca.2011.11.036
30. Lee G, Lee HY, Park H, et al. Radiomics and its emerging role in lung cancer research, imaging biomarkers and clinical management: state of the art. *Eur J Radiol*. 2017;86:297–307. doi:10.1016/j.ejrad.2016.09.005
31. Cook GJR, Azad G, Owczarczyk K, Siddique M, Goh V. Challenges and Promises of PET Radiomics. *Int J Radiat Oncol Biol Phys*. 2018;102(4):1083–1089. doi:10.1016/j.ijrobp.2017.12.268
32. Gillies RJ, Kinahan PE, Hricak H. Radiomics: images Are More than Pictures, They Are Data. *Radiology*. 2016;278(2):563–577. doi:10.1148/radiol.2015151169
33. Papp L, Rausch I, Grahovac M, Hacker M, Beyer T. Optimized Feature Extraction for Radiomics Analysis of (18)F-FDG PET Imaging. *J Nucl Med*. 2019;60(6):864–872. doi:10.2967/jnumed.118.217612
34. Sollini M, Cozzi L, Antunovic L, Chiti A, Kirienko M. PET Radiomics in NSCLC: state of the art and a proposal for harmonization of methodology. *Sci Rep*. 2017;7(1):358. doi:10.1038/s41598-017-00426-y
35. Jirák D, Dezortová M, Taimr P, Hájek M. Texture analysis of human liver. *J Magn Reson Imaging*. 2002;15(1):68–74. doi:10.1002/jmri.10042
36. Zwanenburg A, Vallières M, Abdalah MA, et al. The Image Biomarker Standardization Initiative: standardized Quantitative Radiomics for High-Throughput Image-based Phenotyping. *Radiology*. 2020;295(2):328–338. doi:10.1148/radiol.2020191145
37. Ha S, Choi H, Paeng JC, Cheon GJ. Radiomics in Oncological PET/CT: a Methodological Overview. *Nucl Med Mol Imaging*. 2019;53(1):14–29. doi:10.1007/s13139-019-00571-4
38. Thibault G, Angulo J, Meyer F. Advanced Statistical Matrices for Texture Characterization: application to Cell Classification. *IEEE Trans Biomed Eng*. 2014;61(3):630–637. doi:10.1109/TBME.2013.2284600
39. Smith TG, Lange GD, Marks WB. Fractal methods and results in cellular morphology--dimensions, lacunarity and multifractals. *J Neurosci Methods*. 1996;69(2):123–136. doi:10.1016/s0165-0270(96)00080-5
40. Lin YC, Lin CH, Lu HY, et al. Deep learning for fully automated tumor segmentation and extraction of magnetic resonance radiomics features in cervical cancer. *Eur Radiol*. 2020;30(3):1297–1305. doi:10.1007/s00330-019-06467-3
41. Avanzo M, Stancanello J, Pirrone G, Sartor G. Radiomics and deep learning in lung cancer. *Strahlenther Onkol*. 2020;196(10):879–887. doi:10.1007/s00066-020-01625-9
42. Park HJ, Park B, Lee SS. Radiomics and Deep Learning: hepatic Applications. *Korean J Radiol*. 2020;21(4):387–401. doi:10.3348/kjr.2019.0752

43. Liu Z, Wang S, Dong D, et al. The Applications of Radiomics in Precision Diagnosis and Treatment of Oncology: opportunities and Challenges. *Theranostics*. 2019;9(5):1303–1322. doi:10.7150/thno.30309
44. Lu B, Chen Y, Park JC, Fan Q, Kahler D, Liu C. A method of surface marker location optimization for tumor motion estimation in lung stereotactic body radiation therapy. *Med Phys*. 2015;42(1):244–253. doi:10.1118/1.4903888
45. Daneshvar A, Mousa G. Regression shrinkage and selection via least quantile shrinkage and selection operator. *PLoS One*. 2023;18(2): e0266267. doi:10.1371/journal.pone.0266267
46. Zhang B, He X, Ouyang F, et al. Radiomic machine-learning classifiers for prognostic biomarkers of advanced nasopharyngeal carcinoma. *Cancer Lett*. 2017;403:21–27. doi:10.1016/j.canlet.2017.06.004
47. Sarica A, Cerasa A, Quattrone A. Random Forest Algorithm for the Classification of Neuroimaging Data in Alzheimer's Disease: a Systematic Review. *Front Aging Neurosci*. 2017;9:329. doi:10.3389/fnagi.2017.00329
48. Lee SM, Tran PL, Li CS. Goodness-of-fit tests for a logistic regression model with missing covariates. *Stat Methods Med Res*. 2022;31 (6):1031–1050. doi:10.1177/09622802221079350
49. Kang C, Huo Y, Xin L, Tian B, Yu B. Feature selection and tumor classification for microarray data using relaxed Lasso and generalized multi-class support vector machine. *J Theor Biol*. 2019;463:77–91. doi:10.1016/j.jtbi.2018.12.010
50. Yuan J, Zhang Y, Wang X. Application of machine learning in the management of lymphoma: current practice and future prospects. *Digit Health*. 2024;10:20552076241247963. doi:10.1177/20552076241247963
51. Mayerhoefer ME, Materka A, Langs G, et al. Introduction to Radiomics. *J Nucl Med*. 2020;61(4):488–495. doi:10.2967/jnumed.118.222893
52. Guo R, Hu X, Song H, et al. Weakly supervised deep learning for determining the prognostic value of (18)F-FDG PET/CT in extranodal natural killer/T cell lymphoma, nasal type. *Eur J Nucl Med Mol Imaging*. 2021;48(10):3151–3161. doi:10.1007/s00259-021-05232-3
53. Miyoshi H, Sato K, Kabeya Y, et al. Deep learning shows the capability of high-level computer-aided diagnosis in malignant lymphoma. *Lab Invest*. 2020;100(10):1300–1310. doi:10.1038/s41374-020-0442-3
54. Dunleavy K. Advances in the management of primary central nervous system lymphoma. *Clin Adv Hematol Oncol*. 2017;15(9):677–679.
55. Cheung MM, Chan JK, Lau WH, Ngan RK, Foo WW. Early stage nasal NK/T-cell lymphoma: clinical outcome, prognostic factors, and the effect of treatment modality. *Int J Radiat Oncol Biol Phys*. 2002;54(1):182–190. doi:10.1016/s0360-3016(02)02916-4
56. Kong Z, Jiang C, Zhu R, et al. (18)F-FDG-PET-based radiomics features to distinguish primary central nervous system lymphoma from glioblastoma. *Neuroimage Clin*. 2019;23:101912. doi:10.1016/j.nicl.2019.101912
57. Ou X, Zhang J, Wang J, et al. Radiomics based on (18) F-FDG PET/CT could differentiate breast carcinoma from breast lymphoma using machine-learning approach: a preliminary study. *Cancer Med*. 2020;9(2):496–506. doi:10.1002/cam4.2711
58. Sibille L, Seifert R, Avramovic N, et al. (18)F-FDG PET/CT Uptake Classification in Lymphoma and Lung Cancer by Using Deep Convolutional Neural Networks. *Radiology*. 2020;294(2):445–452. doi:10.1148/radiol.2019191114
59. Cui C, Yao X, Xu L, et al. Improving the Classification of PCNSL and Brain Metastases by Developing a Machine Learning Model Based on (18)F-FDG PET. *J Pers Med*. 2023;13(3):539. doi:10.3390/jpm13030539
60. Wang J, Zhou Y, Zhou J, Liu H, Li X. Preliminary study on the ability of the machine learning models based on (18)F-FDG PET/CT to differentiate between mass-forming pancreatic lymphoma and pancreatic carcinoma. *Eur J Radiol*. 2024;176:111531. doi:10.1016/j.ejrad.2024.111531
61. Zhu S, Xu H, Shen C, et al. Differential diagnostic ability of 18F-FDG PET/CT radiomics features between renal cell carcinoma and renal lymphoma. *Q J Nucl Med Mol Imaging*. 2021;65(1):72–78. doi:10.23736/s1824-4785.19.03137-6
62. Lovinfosse P, Ferreira M, Withofs N, et al. Distinction of Lymphoma from Sarcoidosis on (18)F-FDG PET/CT: evaluation of Radiomics-Feature-Guided Machine Learning Versus Human Reader Performance. *J Nucl Med*. 2022;63(12):1933–1940. doi:10.2967/jnumed.121.263598
63. Mayerhoefer ME, Riedl CC, Kumar A, et al. [18F]FDG-PET/CT Radiomics for Prediction of Bone Marrow Involvement in Mantle Cell Lymphoma: a Retrospective Study in 97 Patients. *Cancers*. 2020;12(5):1138. doi:10.3390/cancers12051138
64. Eertink JJ, van de Brug T, Wiegers SE, et al. (18)F-FDG PET baseline radiomics features improve the prediction of treatment outcome in diffuse large B-cell lymphoma. *Eur J Nucl Med Mol Imaging*. 2022;49(3):932–942. doi:10.1007/s00259-021-05480-3
65. Ortega C, Eshet Y, Prica A, et al. Combination of FDG PET/CT Radiomics and Clinical Parameters for Outcome Prediction in Patients with Hodgkin's Lymphoma. *Cancers*. 2023;15(7):2056. doi:10.3390/cancers15072056
66. Swerdlow SH, Campo E, Pileri SA, et al. The 2016 revision of the World Health Organization classification of lymphoid neoplasms. *Blood*. 2016;127(20):2375–2390. doi:10.1182/blood-2016-01-643569
67. Abenavoli EM, Barbetti M, Linguanti F, et al. Characterization of Mediastinal Bulky Lymphomas with FDG-PET-Based Radiomics and Machine Learning Techniques. *Cancers*. 2023;15(7):1931. doi:10.3390/cancers15071931
68. Lippi M, Gianotti S, Fama A, et al. Texture analysis and multiple-instance learning for the classification of malignant lymphomas. *Comput Methods Programs Biomed*. 2020;185:105153. doi:10.1016/j.cmpb.2019.105153
69. Diao Z, Jiang H. A multi-instance tumor subtype classification method for small PET datasets using RA-DL attention module guided deep feature extraction with radiomics features. *Comput Biol Med*. 2024;174:108461. doi:10.1016/j.compbiomed.2024.108461
70. Wang M, Jiang H. PST-Radiomics: a PET/CT lymphoma classification method based on pseudo spatial-temporal radiomic features and structured atrous recurrent convolutional neural network. *Phys Med Biol*. 2023;68(23):235014. doi:10.1088/1361-6560/ad0c0f
71. Al-Tourah AJ, Gill KK, Chhanabhai M, et al. Population-based analysis of incidence and outcome of transformed non-Hodgkin's lymphoma. *J Clin Oncol*. 2008;26(32):5165–5169. doi:10.1200/jco.2008.16.0283
72. Montoto S, Davies AJ, Matthews J, et al. Risk and clinical implications of transformation of follicular lymphoma to diffuse large B-cell lymphoma. *J Clin Oncol*. 2007;25(17):2426–2433. doi:10.1200/jco.2006.09.3260
73. Freedman AS. Biology and management of histologic transformation of indolent lymphoma. *Hematology Am Soc Hematol Educ Program*. 2005;2005:314–320. doi:10.1182/asheducation-2005.1.314
74. Parikh SA, Kay NE, Shanafelt TD. How we treat Richter syndrome. *Blood*. 2014;123(11):1647–1657. doi:10.1182/blood-2013-11-516229
75. Ayers EC, Mato AR. Richter's Transformation in the Era of Kinase Inhibitor Therapy: a Review. *Clin Lymphoma Myeloma Leuk*. 2017;17 (1):1–6. doi:10.1016/j.clml.2016.08.021

76. Rossi D. Richter's syndrome: novel and promising therapeutic alternatives. *Best Pract Res Clin Haematol*. 2016;29(1):30–39. doi:10.1016/j.beha.2016.08.006
77. Cerhan JR, Slager SL. Familial predisposition and genetic risk factors for lymphoma. *Blood*. 2015;126(20):2265–2273. doi:10.1182/blood-2015-04-537498
78. Suarez F, Lecuit M. Infection-associated non-Hodgkin lymphomas. *Clin Microbiol Infect*. 2015;21(11):991–997. doi:10.1016/j.cmi.2015.07.020
79. Condoluci A, Rossi D. Biology and Treatment of Richter Transformation. *Front Oncol*. 2022;12:829983. doi:10.3389/fonc.2022.829983
80. Khan M, Siddiqi R, Thompson PA. Approach to Richter transformation of chronic lymphocytic leukemia in the era of novel therapies. *Ann Hematol*. 2018;97(1):1–15. doi:10.1007/s00277-017-3149-9
81. Thompson PA, Siddiqi T. Treatment of Richter's syndrome. *Hematology Am Soc Hematol Educ Program*. 2022;2022(1):329–336. doi:10.1182/hematology.2022000345
82. Briski R, Taylor J. Treatment of Richter Transformation of Chronic Lymphocytic Leukemia in the Modern Era. *Cancers*. 2023;15(6):1857. doi:10.3390/cancers15061857
83. Michallet AS, Sesques P, Rabe KG, et al. An 18F-FDG-PET maximum standardized uptake value > 10 represents a novel valid marker for discerning Richter's Syndrome. *Leuk Lymphoma*. 2016;57(6):1474–1477. doi:10.3109/10428194.2015.1099643
84. Pontoizeau C, Girard A, Mesbah H, et al. Prognostic Value of Baseline Total Metabolic Tumor Volume Measured on FDG PET in Patients With Richter Syndrome. *Clin Nucl Med*. 2020;45(2):118–122. doi:10.1097/rlu.0000000000002879
85. Hod K, Tova Y, Gold O, et al. The Pattern of Use of PET/CT Scans in the Clinical Management of Chronic Lymphocytic Leukemia. *Clin Lymphoma Myeloma Leuk*. 2021;21(8):558–563. doi:10.1016/j.clml.2021.04.003
86. Bruzzi JF, Macapinlac H, Tsimberidou AM, et al. Detection of Richter's transformation of chronic lymphocytic leukemia by PET/CT. *J Nucl Med*. 2006;47(8):1267–1273.
87. Albano D, Camoni L, Rodella C, Giubbini R, Bertagna F. 2-[(18)F]-FDG PET/CT Role in Detecting Richter Transformation of Chronic Lymphocytic Leukemia and Predicting Overall Survival. *Clin Lymphoma Myeloma Leuk*. 2021;21(3):e277–e283. doi:10.1016/j.clml.2020.12.003
88. Papajík T, Mysliveček M, Urbanová R, et al. 2-[18F]fluoro-2-deoxy-D-glucose positron emission tomography/computed tomography examination in patients with chronic lymphocytic leukemia may reveal Richter transformation. *Leuk Lymphoma*. 2014;55(2):314–319. doi:10.3109/10428194.2013.802313
89. Albano D, Rizzo A, Racca M, Muoio B, Bertagna F, Treglia G. The Diagnostic Performance of 2-[(18)F]FDG PET/CT in Identifying Richter Transformation in Chronic Lymphocytic Leukemia: an Updated Systematic Review and Bivariate Meta-Analysis. *Cancers*. 2024;16(9):1778. doi:10.3390/cancers16091778
90. Albano D, Calabrò A, Dondi F, Bertagna F. 2-[(18)F]-FDG PET/CT Semiquantitative and Radiomics Predictive Parameters of Richter's Transformation in CLL Patients. *Medicina*. 2024;60(2):203. doi:10.3390/medicina60020203
91. Wondergem MJ, Rizvi SN, Jauw Y, et al. 18F-FDG or 3'-deoxy-3'-18F-fluorothymidine to detect transformation of follicular lymphoma. *J Nucl Med*. 2015;56(2):216–221. doi:10.2967/jnumed.114.149625
92. Karam M, Feustel PJ, Vera CD, Nazeer T. Features of large cell transformation of indolent lymphomas as observed on sequential PET/CT. *Nucl Med Commun*. 2011;32(3):177–185. doi:10.1097/MNM.0b013e328342b9d2
93. Karam M, Novak L, Cyriac J, Ali A, Nazeer T, Nugent F. Role of fluorine-18 fluoro-deoxyglucose positron emission tomography scan in the evaluation and follow-up of patients with low-grade lymphomas. *Cancer*. 2006;107(1):175–183. doi:10.1002/cncr.21967
94. Bodet-Milin C, Kraeber-Bodéré F, Moreau P, Campion L, Dupas B, Le Gouill S. Investigation of FDG-PET/CT imaging to guide biopsies in the detection of histological transformation of indolent lymphoma. *Haematologica*. 2008;93(3):471–472. doi:10.3324/haematol.12013
95. Mir F, Barrington SF, Brown H, et al. Baseline SUVmax did not predict histological transformation in follicular lymphoma in the Phase 3 GALLIUM study. *Blood*. 2020;135(15):1214–1218. doi:10.1182/blood.2019001091
96. Fletcher JW, Djulbegovic B, Soares HP, et al. Recommendations on the use of 18F-FDG PET in oncology. *J Nucl Med*. 2008;49(3):480–508. doi:10.2967/jnumed.107.047787
97. Hutchings M, Loft A, Hansen M, et al. Position emission tomography with or without computed tomography in the primary staging of Hodgkin's lymphoma. *Haematologica*. 2006;91(4):482–489.
98. Pelosi E, Pregno P, Penna D, et al. Role of whole-body [18F] fluorodeoxyglucose positron emission tomography/computed tomography (FDG-PET/CT) and conventional techniques in the staging of patients with Hodgkin and aggressive non Hodgkin lymphoma. *Radiol Med*. 2008;113(4):578–590. doi:10.1007/s11547-008-0264-7
99. Le Dortz L, De Guibert S, Bayat S, et al. Diagnostic and prognostic impact of 18F-FDG PET/CT in follicular lymphoma. *Eur J Nucl Med Mol Imaging*. 2010;37(12):2307–2314. doi:10.1007/s00259-010-1539-5
100. Jerusalem G, Beguin Y, Fassotte MF, et al. Whole-body positron emission tomography using 18F-fluorodeoxyglucose compared to standard procedures for staging patients with Hodgkin's disease. *Haematologica*. 2001;86(3):266–273.
101. Fuertes S, Setoain X, López-Guillermo A, et al. Utilidad de la tomografía por emisión de positrones/ tomografía computarizada (PET/TC) en el estudio de extensión en pacientes con linfoma B difuso de células grandes [The value of positron emission tomography/computed tomography (PET/CT) in the staging of diffuse large B-cell lymphoma]. *Med Clin*. 2007;129(18):688–693. doi:10.1157/13112510
102. Janikova A, Bolcak K, Pavlik T, Mayer J, Kral Z. Value of [18F]fluorodeoxyglucose positron emission tomography in the management of follicular lymphoma: the end of a dilemma? *Clin Lymphoma Myeloma*. 2008;8(5):287–293. doi:10.3816/CLM.2008.n.040
103. Wirth A, Foo M, Seymour JF, Macmanus MP, Hicks RJ. Impact of [18f] fluorodeoxyglucose positron emission tomography on staging and management of early-stage follicular non-Hodgkin lymphoma. *Int J Radiat Oncol Biol Phys*. 2008;71(1):213–219. doi:10.1016/j.ijrobp.2007.09.051
104. Casulo C, Schöder H, Feeney J, et al. 18F-fluorodeoxyglucose positron emission tomography in the staging and prognosis of T cell lymphoma. *Leuk Lymphoma*. 2013;54(10):2163–2167. doi:10.3109/10428194.2013.767901
105. Carr R, Barrington SF, Madan B, et al. Detection of lymphoma in bone marrow by whole-body positron emission tomography. *Blood*. 1998;91(9):3340–3346.
106. Moog F, Bangerter M, Kotzerke J, Guhlmann A, Frickhofen N, Reske SN. 18-F-fluorodeoxyglucose-positron emission tomography as a new approach to detect lymphomatous bone marrow. *J Clin Oncol*. 1998;16(2):603–609. doi:10.1200/jco.1998.16.2.603

107. Wang J, Weiss LM, Chang KL, et al. Diagnostic utility of bilateral bone marrow examination: significance of morphologic and ancillary technique study in malignancy. *Cancer*. 2002;94(5):1522–1531. doi:10.1002/cncr.10364
108. Franco V, Tripodo C, Rizzo A, Stella M, Florena AM. Bone marrow biopsy in Hodgkin's lymphoma. *Eur J Haematol*. 2004;73(3):149–155. doi:10.1111/j.1600-0609.2004.00292.x
109. Arber DA, George TI. Bone marrow biopsy involvement by non-Hodgkin's lymphoma: frequency of lymphoma types, patterns, blood involvement, and discordance with other sites in 450 specimens. *Am J Surg Pathol*. 2005;29(12):1549–1557. doi:10.1097/01.pas.0000182405.65041.8b
110. Hosein PJ, Pastorini VH, Paes FM, et al. Utility of positron emission tomography scans in mantle cell lymphoma. *Am J Hematol*. 2011;86(10):841–845. doi:10.1002/ajh.22126
111. Bodet-Milin C, Touzeau C, Leux C, et al. Prognostic impact of 18F-fluoro-deoxyglucose positron emission tomography in untreated mantle cell lymphoma: a retrospective study from the GOELAMS group. *Eur J Nucl Med Mol Imaging*. 2010;37(9):1633–1642. doi:10.1007/s00259-010-1469-2
112. Albano D, Ferro P, Bosio G, et al. Diagnostic and Clinical Impact of Staging (18)F-FDG PET/CT in Mantle-Cell Lymphoma: a Two-Center Experience. *Clin Lymphoma Myeloma Leuk*. 2019;19(8):e457–e464. doi:10.1016/j.clml.2019.04.016
113. Dreyling M, Ghielmini M, Marcus R, Salles G, Vitolo U. Newly diagnosed and relapsed follicular lymphoma: ESMO Clinical Practice Guidelines for diagnosis, treatment and follow-up. *Ann Oncol*. 2011;22 Suppl 6:vi59–63. doi:10.1093/annonc/mdr388
114. Asenbaum U, Nolz R, Karanikas G, et al. Bone Marrow Involvement in Malignant Lymphoma: evaluation of Quantitative PET and MRI Biomarkers. *Acad Radiol*. 2018;25(4):453–460. doi:10.1016/j.acra.2017.10.024
115. Morgan R, Perry M, Kwak J, Jensen A, Kamdar M. Positron Emission Tomography-based Analysis Can Accurately Predict Bone Marrow Involvement With Mantle Cell Lymphoma. *Clin Lymphoma Myeloma Leuk*. 2018;18(11):731–736. doi:10.1016/j.clml.2018.06.024
116. Adams HJ, Kwee TC, Fijnheer R, et al. Utility of quantitative FDG-PET/CT for the detection of bone marrow involvement in follicular lymphoma: a histopathological correlation study. *Skeletal Radiol*. 2014;43(9):1231–1236. doi:10.1007/s00256-014-1919-1
117. Adams HJ, Kwee TC, Fijnheer R, Dubois SV, Nievelstein RA, de Klerk JM. Direct comparison of visual and quantitative bone marrow FDG-PET/CT findings with bone marrow biopsy results in diffuse large B-cell lymphoma: does bone marrow FDG-PET/CT live up to its promise? *Acta Radiol*. 2015;56(10):1230–1235. doi:10.1177/0284185114554824
118. Aide N, Talbot M, Fruchart C, Damaj G, Lasnon C. Diagnostic and prognostic value of baseline FDG PET/CT skeletal textural features in diffuse large B cell lymphoma. *Eur J Nucl Med Mol Imaging*. 2018;45(5):699–711. doi:10.1007/s00259-017-3899-6
119. Kenawy MA, Khalil MM, Abdelgawad MH, El-Bahnasawy HH. Correlation of texture feature analysis with bone marrow infiltration in initial staging of patients with lymphoma using (18)F-fluorodeoxyglucose positron emission tomography combined with computed tomography. *Pol J Radiol*. 2020;85:e586–e594. doi:10.5114/pjr.2020.99833
120. International Non-Hodgkin's Lymphoma Prognostic Factors Project. A predictive model for aggressive non-Hodgkin's lymphoma. *N Engl J Med*. 1993;329(14):987–994. doi:10.1056/nejm199309303291402
121. Sehn LH, Berry B, Chhanabhai M, et al. The revised International Prognostic Index (R-IPI) is a better predictor of outcome than the standard IPI for patients with diffuse large B-cell lymphoma treated with R-CHOP. *Blood*. 2007;109(5):1857–1861. doi:10.1182/blood-2006-08-038257
122. Zhou Z, Sehn LH, Rademaker AW, et al. An enhanced International Prognostic Index (NCCN-IPI) for patients with diffuse large B-cell lymphoma treated in the rituximab era. *Blood*. 2014;123(6):837–842. doi:10.1182/blood-2013-09-524108
123. Gleeson M, Counsell N, Cunningham D, et al. Prognostic indices in diffuse large B-cell lymphoma in the rituximab era: an analysis of the UK National Cancer Research Institute R-CHOP 14 versus 21 phase 3 trial. *Br J Haematol*. 2021;192(6):1015–1019. doi:10.1111/bjh.16691
124. Ruppert AS, Dixon JG, Salles G, et al. International prognostic indices in diffuse large B-cell lymphoma: a comparison of IPI, R-IPI, and NCCN-IPI. *Blood*. 2020;135(23):2041–2048. doi:10.1182/blood.2019002729
125. Zhang X, Chen L, Jiang H, et al. A novel analytic approach for outcome prediction in diffuse large B-cell lymphoma by [(18)F]FDG PET/CT. *Eur J Nucl Med Mol Imaging*. 2022;49(4):1298–1310. doi:10.1007/s00259-021-05572-0
126. Cottereau AS, Nioche C, Dirand AS, et al. (18)F-FDG PET Dissemination Features in Diffuse Large B-Cell Lymphoma Are Predictive of Outcome. *J Nucl Med*. 2020;61(1):40–45. doi:10.2967/jnumed.119.229450
127. Ceriani L, Gritti G, Cascione L, et al. SAKK38/07 study: integration of baseline metabolic heterogeneity and metabolic tumor volume in DLBCL prognostic model. *Blood Adv*. 2020;4(6):1082–1092. doi:10.1182/bloodadvances.2019001201
128. Engert A, Plütschow A, Eich HT, et al. Reduced treatment intensity in patients with early-stage Hodgkin's lymphoma. *N Engl J Med*. 2010;363(7):640–652. doi:10.1056/NEJMoa1000067
129. Eich HT, Diehl V, Görgen H, et al. Intensified chemotherapy and dose-reduced involved-field radiotherapy in patients with early unfavorable Hodgkin's lymphoma: final analysis of the German Hodgkin Study Group HD11 trial. *J Clin Oncol*. 2010;28(27):4199–4206. doi:10.1200/jco.2010.29.8018
130. Moskowitz CH, Kewalramani T, Nimer SD, Gonzalez M, Zelenetz AD, Yahalom J. Effectiveness of high dose chemoradiotherapy and autologous stem cell transplantation for patients with biopsy-proven primary refractory Hodgkin's disease. *Br J Haematol*. 2004;124(5):645–652. doi:10.1111/j.1365-2141.2003.04828.x
131. Specht L, Nordentoft AM, Cold S, Clausen NT, Nissen NI. Tumor burden as the most important prognostic factor in early stage Hodgkin's disease. Relations to other prognostic factors and implications for choice of treatment. *Cancer*. 1988;61(8):1719–1727. doi:10.1002/1097-0142(19880415)61:8<1719::aid-cncr2820610834>3.0.co;2-a
132. Akhtari M, Milgrom SA, Pinnix CC, et al. Reclassifying patients with early-stage Hodgkin lymphoma based on functional radiographic markers at presentation. *Blood*. 2018;131(1):84–94. doi:10.1182/blood-2017-04-773838
133. Cottereau AS, Versari A, Loft A, et al. Prognostic value of baseline metabolic tumor volume in early-stage Hodgkin lymphoma in the standard arm of the H10 trial. *Blood*. 2018;131(13):1456–1463. doi:10.1182/blood-2017-07-795476
134. Fermé C, Eghbali H, Meerwaldt JH, et al. Chemotherapy plus involved-field radiation in early-stage Hodgkin's disease. *N Engl J Med*. 2007;357(19):1916–1927. doi:10.1056/NEJMoa064601
135. Sieber M, Engert A, Diehl V. Treatment of Hodgkin's disease: results and current concepts of the German Hodgkin's Lymphoma Study Group. *Ann Oncol*. 2000;11 Suppl 1:81–85.

136. Hoppe RT, Advani RH, Ai WZ, et al. Hodgkin lymphoma, version 2.2015. *J Natl Compr Canc Netw*. 2015;13(5):554–586. doi:10.6004/jnccn.2015.0075
137. Triumbari EKA, Morland D, Cuccaro A, Maiolo E, Hohaus S, Annunziata S. Classical Hodgkin Lymphoma: a Joint Clinical and PET Model to Predict Poor Responders at Interim Assessment. *Diagnostics*. 2022;12(10):2325. doi:10.3390/diagnostics12102325
138. Triumbari EKA, Gatta R, Maiolo E, et al. Baseline (18)F-FDG PET/CT Radiomics in Classical Hodgkin's Lymphoma: the Predictive Role of the Largest and the Hottest Lesions. *Diagnostics*. 2023;13(8):1391. doi:10.3390/diagnostics13081391
139. Yim SK, Yhim HY, Han YH, et al. Early risk stratification for diffuse large B-cell lymphoma integrating interim Deauville score and International Prognostic Index. *Ann Hematol*. 2019;98(12):2739–2748. doi:10.1007/s00277-019-03834-4
140. Wight JC, Chong G, Grigg AP, Hawkes EA. Prognostication of diffuse large B-cell lymphoma in the molecular era: moving beyond the IPI. *Blood Rev*. 2018;32(5):400–415. doi:10.1016/j.blre.2018.03.005
141. Miyazaki Y, Nawa Y, Miyagawa M, et al. Maximum standard uptake value of 18F-fluorodeoxyglucose positron emission tomography is a prognostic factor for progression-free survival of newly diagnosed patients with diffuse large B cell lymphoma. *Ann Hematol*. 2013;92(2):239–244. doi:10.1007/s00277-012-1602-3
142. Chang CC, Cho SF, Tu HP, et al. Tumor and bone marrow uptakes on [18F]fluorodeoxyglucose positron emission tomography/computed tomography predict prognosis in patients with diffuse large B-cell lymphoma receiving rituximab-containing chemotherapy. *Medicine*. 2017;96(45):e8655. doi:10.1097/md.0000000000008655
143. Albano D, Mazzoletti A, Spallino M, et al. Prognostic role of baseline 18F-FDG PET/CT metabolic parameters in elderly HL: a two-center experience in 123 patients. *Ann Hematol*. 2020;99(6):1321–1330. doi:10.1007/s00277-020-04039-w
144. Angelopoulou MK, Mosa E, Pangalis GA, et al. The Significance of PET/CT in the Initial Staging of Hodgkin Lymphoma: experience Outside Clinical Trials. *Anticancer Res*. 2017;37(10):5727–5736. doi:10.21873/anticanres.12011
145. Chihara D, Oki Y, Onoda H, et al. High maximum standard uptake value (SUVmax) on PET scan is associated with shorter survival in patients with diffuse large B cell lymphoma. *Int J Hematol*. 2011;93(4):502–508. doi:10.1007/s12185-011-0822-y
146. Xia X, Wang Y, Yuan J, et al. Baseline SUVmax of 18F-FDG PET-CT indicates prognosis of extranodal natural killer/T-cell lymphoma. *Medicine*. 2020;99(37):e22143. doi:10.1097/md.0000000000022143
147. Adams MC, Turkington TG, Wilson JM, Wong TZ. A systematic review of the factors affecting accuracy of SUV measurements. *AJR Am J Roentgenol*. 2010;195(2):310–320. doi:10.2214/ajr.10.4923
148. Kinahan PE, Fletcher JW. Positron emission tomography-computed tomography standardized uptake values in clinical practice and assessing response to therapy. *Semin Ultrasound CT MR*. 2010;31(6):496–505. doi:10.1053/j.sult.2010.10.001
149. Vercellino L, Cottereau AS, Casasnovas O, et al. High total metabolic tumor volume at baseline predicts survival independent of response to therapy. *Blood*. 2020;135(16):1396–1405. doi:10.1182/blood.2019003526
150. Dean EA, Mhaskar RS, Lu H, et al. High metabolic tumor volume is associated with decreased efficacy of axicabtagene ciloleucel in large B-cell lymphoma. *Blood Adv*. 2020;4(14):3268–3276. doi:10.1182/bloodadvances.2020001900
151. Mehta-Shah N, Ito K, Bantilan K, et al. Baseline and interim functional imaging with PET effectively risk stratifies patients with peripheral T-cell lymphoma. *Blood Adv*. 2019;3(2):187–197. doi:10.1182/bloodadvances.2018024075
152. Thieblemont C, Chartier L, Dührsen U, et al. A tumor volume and performance status model to predict outcome before treatment in diffuse large B-cell lymphoma. *Blood Adv*. 2022;6(23):5995–6004. doi:10.1182/bloodadvances.2021006923
153. Cottereau AS, Lanic H, Mareschal S, et al. Molecular Profile and FDG-PET/CT Total Metabolic Tumor Volume Improve Risk Classification at Diagnosis for Patients with Diffuse Large B-Cell Lymphoma. *Clin Cancer Res*. 2016;22(15):3801–3809. doi:10.1158/1078-0432.Ccr-15-2825
154. Voltin CA, Mettler J, van Heek L, et al. Early Response to First-Line Anti-PD-1 Treatment in Hodgkin Lymphoma: a PET-Based Analysis from the Prospective, Randomized Phase II NIVAHL Trial. *Clin Cancer Res*. 2021;27(2):402–407. doi:10.1158/1078-0432.Ccr-20-3303
155. Burggraaff CN, Eertink JJ, Lugtenburg PJ, et al. (18)F-FDG PET Improves Baseline Clinical Predictors of Response in Diffuse Large B-Cell Lymphoma: the HOVON-84 Study. *J Nucl Med*. 2022;63(7):1001–1007. doi:10.2967/jnumed.121.262205
156. Moskowitz CH. Interim PET-CT in the management of diffuse large B-cell lymphoma. *Hematology Am Soc Hematol Educ Program*. 2012;2012:397–401. doi:10.1182/asheducation-2012.1.397
157. Song MK, Chung JS, Shin HJ, et al. Clinical significance of metabolic tumor volume by PET/CT in stages II and III of diffuse large B cell lymphoma without extranodal site involvement. *Ann Hematol*. 2012;91(5):697–703. doi:10.1007/s00277-011-1357-2
158. Kim TM, Paeng JC, Chun IK, et al. Total lesion glycolysis in positron emission tomography is a better predictor of outcome than the International Prognostic Index for patients with diffuse large B cell lymphoma. *Cancer*. 2013;119(6):1195–1202. doi:10.1002/cncr.27855
159. Kanoun S, Rossi C, Berriolo-Riedinger A, et al. Baseline metabolic tumour volume is an independent prognostic factor in Hodgkin lymphoma. *Eur J Nucl Med Mol Imaging*. 2014;41(9):1735–1743. doi:10.1007/s00259-014-2783-x
160. Kostakoglu L, Mattiello F, Martelli M, et al. Total metabolic tumor volume as a survival predictor for patients with diffuse large B-cell lymphoma in the GOYA study. *Haematologica*. 2022;107(7):1633–1642. doi:10.3324/haematol.2021.278663
161. Gallicchio R, Mansueto G, Simeon V, et al. F-18 FDG PET/CT quantization parameters as predictors of outcome in patients with diffuse large B-cell lymphoma. *Eur J Haematol*. 2014;92(5):382–389. doi:10.1111/ejh.12268
162. Hussien AE, Furth C, Schönberger S, et al. FDG-PET Response Prediction in Pediatric Hodgkin's Lymphoma: impact of Metabolically Defined Tumor Volumes and Individualized SUV Measurements on the Positive Predictive Value. *Cancers*. 2015;7(1):287–304. doi:10.3390/cancers7010287
163. Capobianco N, Meignan M, Cottereau AS, et al. Deep-Learning (18)F-FDG Uptake Classification Enables Total Metabolic Tumor Volume Estimation in Diffuse Large B-Cell Lymphoma. *J Nucl Med*. 2021;62(1):30–36. doi:10.2967/jnumed.120.242412
164. Moskowitz AJ, Schöder H, Gavane S, et al. Prognostic significance of baseline metabolic tumor volume in relapsed and refractory Hodgkin lymphoma. *Blood*. 2017;130(20):2196–2203. doi:10.1182/blood-2017-06-788877
165. Procházka V, Gawande RS, Cayci Z, et al. Positron Emission Tomography-Based Assessment of Metabolic Tumor Volume Predicts Survival after Autologous Hematopoietic Cell Transplantation for Hodgkin Lymphoma. *Biol Blood Marrow Transplant*. 2018;24(1):64–70. doi:10.1016/j.bbmt.2017.09.006
166. Voorhees TJ, Zhao B, Oldan J, et al. Pretherapy metabolic tumor volume is associated with response to CD30 CAR T cells in Hodgkin lymphoma. *Blood Adv*. 2022;6(4):1255–1263. doi:10.1182/bloodadvances.2021005385

167. Meignan M, Cottereau AS, Versari A, et al. Baseline Metabolic Tumor Volume Predicts Outcome in High-Tumor-Burden Follicular Lymphoma: a Pooled Analysis of Three Multicenter Studies. *J Clin Oncol*. 2016;34(30):3618–3626. doi:10.1200/jco.2016.66.9440
168. Delfau-Larue MH, van der Gucht A, Dupuis J, et al. Total metabolic tumor volume, circulating tumor cells, cell-free DNA: distinct prognostic value in follicular lymphoma. *Blood Adv*. 2018;2(7):807–816. doi:10.1182/bloodadvances.2017015164
169. Guo B, Tan X, Ke Q, Cen H. Prognostic value of baseline metabolic tumor volume and total lesion glycolysis in patients with lymphoma: a meta-analysis. *PLoS One*. 2019;14(1):e0210224. doi:10.1371/journal.pone.0210224
170. Cottereau AS, Meignan M, Nioche C, et al. Risk stratification in diffuse large B-cell lymphoma using lesion dissemination and metabolic tumor burden calculated from baseline PET/CT(†). *Ann Oncol*. 2021;32(3):404–411. doi:10.1016/j.annonc.2020.11.019
171. Ceriani L, Milan L, Martelli M, et al. Metabolic heterogeneity on baseline 18FDG-PET/CT scan is a predictor of outcome in primary mediastinal B-cell lymphoma. *Blood*. 2018;132(2):179–186. doi:10.1182/blood-2018-01-826958
172. Aide N, Fruchart C, Nganoa C, Gac AC, Lasnon C. Baseline (18)F-FDG PET radiomic features as predictors of 2-year event-free survival in diffuse large B cell lymphomas treated with immunochemotherapy. *Eur Radiol*. 2020;30(8):4623–4632. doi:10.1007/s00330-020-06815-8
173. Ritter Z, Papp L, Zámbó K, et al. Two-Year Event-Free Survival Prediction in DLBCL Patients Based on In Vivo Radiomics and Clinical Parameters. *Front Oncol*. 2022;12:820136. doi:10.3389/fonc.2022.820136
174. Frood R, Clark M, Burton C, et al. Discovery of Pre-Treatment FDG PET/CT-Derived Radiomics-Based Models for Predicting Outcome in Diffuse Large B-Cell Lymphoma. *Cancers*. 2022;14(7):1711. doi:10.3390/cancers14071711
175. Gallamini A, Rambaldi A, Patti C, et al. Lesion Dissemination in Baseline PET/CT (D-MAX) and IPS Score Predict ABVD Treatment Outcome in PET-2 Negative Advanced-Stage Hodgkin Lymphoma Patients Enrolled in the Prospective GITIL/FIL HD0607 Trial. *Blood*. 2021;138:2443. doi:10.1182/blood-2021-152292
176. Frood R, Clark M, Burton C, et al. Utility of pre-treatment FDG PET/CT-derived machine learning models for outcome prediction in classical Hodgkin lymphoma. *Eur Radiol*. 2022;32(10):7237–7247. doi:10.1007/s00330-022-09039-0
177. Milgrom SA, Elhalawani H, Lee J, et al. A PET Radiomics Model to Predict Refractory Mediastinal Hodgkin Lymphoma. *Sci Rep*. 2019;9(1):1322. doi:10.1038/s41598-018-37197-z
178. Albano D, Treglia G, Dondi F, et al. 18)F-FDG PET/CT Maximum Tumor Dissemination (Dmax) in Lymphoma: a New Prognostic Factor? *Cancers*. 2023;15(9):2494. doi:10.3390/cancers15092494
179. Cottereau AS, Meignan M, Nioche C, et al. New Approaches in Characterization of Lesions Dissemination in DLBCL Patients on Baseline PET/CT. *Cancers*. 2021;13(16):3998. doi:10.3390/cancers13163998
180. El Naqa I, Grigsby P, Apte A, et al. Exploring feature-based approaches in PET images for predicting cancer treatment outcomes. *Pattern Recognit*. 2009;42(6):1162–1171. doi:10.1016/j.patcog.2008.08.011
181. Tixier F, Vriens D, Cheze-Le Rest C, et al. Comparison of Tumor Uptake Heterogeneity Characterization Between Static and Parametric 18F-FDG PET Images in Non-Small Cell Lung Cancer. *J Nucl Med*. 2016;57(7):1033–1039. doi:10.2967/jnumed.115.166918
182. Yoon HJ, Kim Y, Kim BS. Intratumoral metabolic heterogeneity predicts invasive components in breast ductal carcinoma in situ. *Eur Radiol*. 2015;25(12):3648–3658. doi:10.1007/s00330-015-3761-9
183. Kang SR, Song HC, Byun BH, et al. Intratumoral Metabolic Heterogeneity for Prediction of Disease Progression After Concurrent Chemoradiotherapy in Patients with Inoperable Stage III Non-Small-Cell Lung Cancer. *Nucl Med Mol Imaging*. 2014;48(1):16–25. doi:10.1007/s13139-013-0231-7
184. Lambin P, Leijenaar RTH, Deist TM, et al. Radiomics: the bridge between medical imaging and personalized medicine. *Nat Rev Clin Oncol*. 2017;14(12):749–762. doi:10.1038/nrclinonc.2017.141
185. Al-Ibraheem A, Abdlkadir AS, Al-Adhami DA, et al. The prognostic utility of (18)F-FDG PET parameters in lymphoma patients under CAR-T-cell therapy: a systematic review and meta-analysis. *Front Immunol*. 2024;15:1424269. doi:10.3389/fimmu.2024.1424269
186. Quartuccio N, Ialuna S, Pulizzi S, D'Oppido D, Nicolosi S, Moreci AM. The Role of [(18)F]FDG PET/CT in Predicting Toxicity in Patients with NHL Treated with CAR-T: a Systematic Review. *Tomography*. 2024;10(6):869–879. doi:10.3390/tomography10060066
187. Zwanenburg A. Radiomics in nuclear medicine: robustness, reproducibility, standardization, and how to avoid data analysis traps and replication crisis. *Eur J Nucl Med Mol Imaging*. 2019;46(13):2638–2655. doi:10.1007/s00259-019-04391-8
188. Mongan J, Moy L, Kahn CE. Checklist for Artificial Intelligence in Medical Imaging (CLAIM): a Guide for Authors and Reviewers. *Radiol Artif Intell*. 2020;2(2):e200029. doi:10.1148/ryai.2020200029
189. Eertink JJ, Zwezerijnen GJC, Wiegers SE, et al. Baseline radiomics features and MYC rearrangement status predict progression in aggressive B-cell lymphoma. *Blood Adv*. 2023;7(2):214–223. doi:10.1182/bloodadvances.2022008629